10. LONG-TERM POWER FADING

The variability of tropospheric radio transmission loss depends upon changes in the atmosphere and upon complex interrelationships between various propagation mechanisms. Short-term variability or "phase interference fading," associated with simultaneously occuring modes of propagation, is discussed in annex V. The effects of this type of fading expected within an hour are allowed for by determining an hourly median rms-carrier-to-rms-noise ratio which defines the grade of service that will be provided. Long-term power fading, identified with the variability of hourly median values of transmission loss, is usually due to slow changes in average atmospheric refraction, in the degree of atmospheric stratification, or in the intensity of refractive index turbulence.

An estimate of the long-term power fading to be expected over a given path is important to insure adequate service over the path. The possibility that unusually high interfering fields may occur for an appreciable fraction of time places restrictions on services operating on the same or adjacent frequencies. The basis for the mainly empirical predictions of long-term variability given here needs to be well understood in order to appreciate their value as well as their limitations.

An increase in atmospheric refraction increases long distance diffraction or forward scatter fields but may lead to multipath fading problems over short paths. Increased turbulence of the atmosphere may result in either an increase or a decrease of radio transmission loss depending on the geometry of a particular path and on the dominance of various propagation mechanisms. Increased stratification favors propagation by reflection from elevated layers and sometimes the guiding of energy by ducts or layers. Such stratification usually increases long-distance fields but may be associated with prolonged fadeouts at short distances.

Just beyond radio line-of-sight, fading rate and fading range depend in a very complex manner on the relative importance of various propagation mechanisms. During periods of layering and ducting in the atmosphere, transmission loss shows a tendency to go into relatively deep fades, with durations from less than a minute to more than an hour. Ordinarily a diffraction signal fades slowly if at all, and the fades are of relatively short duration and very deep. A tropospheric forward scatter signal, on the other hand, exhibits the rapid and severe fading characteristic of the Rayleigh distribution. An intermediate type of fading results when the scattered power is nearly equal to power introduced by some mechanism such as diffraction, for which the variation in time is usually very slow. Aircraft reflections introduce rapid, intense, and relatively regular fading. Meteor bursts and some types of ionospheric propagation add spikes to a paper chart record.

Space-wave fadeouts [Bean, 1954] may represent power fading due to defocusing of radio energy in some regions of space, (radio holes) accompanied by a focusing effect and

signal enhancement in other regions [Doherty, 1952; Price, 1948], or may correspond to phase interference fading phenomena. In temperate continental climates, space-wave fadeouts are likely to occur primarily at night and most frequently during the summer months; they are more frequent at UHF than at VHF, and their occurrence can be correlated with the occurrence of ground-modified refractive index profiles [Barsis and Johnson, 1962]. Such fading predominates in geographic areas where layers and ducts occur frequently. Ordinary space diversity does not appear to be helpful in overcoming this type of fading. During periods of uniform refractive-index lapse rates, prolonged fadeouts are much less intense or do not exist. Sometimes those that do exist are caused by multipath reflections which arrive in such a phase and amplitude relationship that a slight change in the lapse rate will cause a large change in the resultant field. The latter type can be overcome in most instances by either relocating the terminal antennas or by the use of space diversity.

General discussions of the time fading of VHF and UHF radio fields will be found in reports by Bullington [1950], du Castel [1957a], Chernov [1955],Grosskopf [1958], Krasil'nikov [1949], Troitski [1957b], and Ugai [1961]. Silverman [1957], discusses some of the theory of the short-term fading of scatter signals, Bremmer [1957] discusses signal distortion due to tropospheric scatter, while Beckmann [1961b] considers related depolarization phenomena.

The observed correlation of radio data with various meteorological parameters is discussed by Bean [1956, 1961], Bean and Cahoon [1957], du Castel and Misme [1957], Josephson and Blomquist [1958], Misme [1958, 1960a, b, c, 1961], Moler and Holden [1960], and Ryde [1946]. Meteorological parameters such as surface refractivity and the height gradient of refractive index have been found more useful as a basis for predicting regional changes than for predicting diurnal or seasonal variations. In this report meteorological information has been used to distinguish between climatic regions, while radio data are depended on to predict long-term variability about the computed long-term median value in each of these regions.

The basic data used in developing these estimates of long-term power fading were recorded in various parts of the world over more than a thousandpropagation paths. Path distances extend from within line-of-sight to about 1000 kilometers, and frequencies range from 40 MHz to 10 GHz.

As more data are collected, particularly in regions where little information is currently available, these estimates should be re-examined and revised. Allowances should sometimes be made for predictable long-term variations in antenna gain, interference due to reflections from aircraft or satellites, and variations in equipment performance. Microwave attenuation due to rainfall, discussed in section 3, should be allowed for in estimating

the variability of transmission loss at frequencies above 5 GHz. The long-term variability of oxygen and water vapor absorption may be important above 15 GHz.

It is often desirable to specify rather precisely the conditions for which an estimate of power fading characteristics is desired. For instance, the average frequency dependence of long-term variability over a given type of profile depends critically on the relative dominance of various propagation mechanisms, and this in turn depends on climate, season, time of day, and average terrain characteristics. When it becomes possible to describe the actual inhomogeneous, stratified, and turbulent atmosphere more adequately, it should also be found worthwhile to "mix" predicted cumulative distributions of transmission loss for a variety of propagation mechanisms.

Three important effects of the atmosphere on radio propagation are considered. The amount a radio ray is bent and the intensity of atmospheric turbulence are usually correlated with the surface refractivity, N_s. The intensity and stability of various types of stratification in the atmosphere are often not well correlated with N_s. Rough terrain and high winds both tend to increase mixing in the atmosphere and consequently reduce the occurrence of superrefractive layers.

10.1 Effects of Atmospheric Stratification

Ground-based superrefractive layers tend to trap radio energy which is propagated within the layer in a manner similar to that in a waveguide. A "normal" gradient of refractive index at the surface of the ground is about -50 N/km, a ground-based superrefractive layer has a gradient from -100 to -157 N/km. Surface layers with stronger negative refractive index gradients may form ducts in which radio energy is refracted to such a degree that it follows the curvature of the earth. If a radio beam is elevated above a minimum angle, usually less than half a degree, the energy penetrates and escapes the duct.

If a transmitter radiating energy in a horizontal direction is located in a duct, the theoretical radio horizon distance over a smooth spherical earth would be infinite. On the other hand in a layer with a subrefractive gradient, (positive values of refractive index gradient) the energy is refracted upwards and the corresponding horizon distance may be much less than that with a normal gradient. For example, a transmitting antenna 50 m above a smooth earth would have a radio horizon distance of about 30 km with a "normal" gradient of about -50 N/km, but the horizon distance might be as little as 8 km under subrefractive conditions or as much as 3 to 5 times the normal distance in a ground-based duct. Such changes would result in marked variations in corresponding values of transmission loss.

The minimum radio frequency that may be trapped by a duct depends on its total thickness and the average refractive index gradient within it. Rather thick, strong ducts will trap frequencies of 300 MHz or less, somewhat weaker and thinner ducts will trap higher frequencies. Frequencies as low as 30 MHz would rarely be trapped. A duct that traps frequencies of about 1000 MHz will guide higher frequencies even more strongly while lower frequencies will exhibit greater attenuation or may not be trapped at all.

It is difficult to predict the fraction of time that high fields due to ducting conditions may be expected to occur. Figures 10.1 to 10.12, which are reproduced from a World Atlas of Atmospheric Radio Refractivity by Bean, Cahoon, Samson and Thayer [1966], show the percentage of time ground-based ducts may occur. These maps are based on radiosonde data recorded at about 100 weather stations, usually for a period of 5 years. The months of February, May, August and November were selected as representative of the seasons. Unfortunately few stations recorded profiles more than once a day so no information on diurnal trends is included. These maps show for frequencies of 300, 1000 and 3000 MHz the percentage of observations in each of the four "seasonal" months that trapping of radio waves may be expected to occur. Such maps indicate general or regional conditions but more information would be required for detailed local predictions.

In large areas of the world, primarily over temperate oceans and arctic areas, the incidence of ducting is less than one percent. Strong ground-based ducts are most common in tropical and subtropical regions from 0° to 30° north latitude, especially in western coastal areas and the Persian Gulf. Strong ducting conditions, for frequencies of 3000 MHz and above and centered on the Persian Gulf may occur as much as 75 percent of the time in

August and only 10 percent of the time in February. In contrast to this on the west coast of Africa, about 15° north latitude, ducting conditions occur about 50 percent of the time in February and November and only 20 to 30 percent of the time in the summer months. Strong subrefractive conditions, with corresponding increased transmission loss, may occur more than 2 percent of the time in tropical Africa, the east coast of South America, the eastern Mediterranean, southeastern Asia and northern Australia.

Some of the better-known maritime areas of superrefraction were listed by Booker [1946]. These include the west coasts of Africa and India, the northern part of the Arabian sea especially around the Persian Gulf in summer, and the northern part of Australia. Particularly during summer months ducting conditions occur in Atlantic coastal areas of Europe, the eastern Mediterranean, the Pacific Coastal areas of China, and in Japan. These early observations of the occurrence of ducting conditions are reflected in the series of world-wide maps, figures 10.1 to 10.12. It is apparent that the most intense superrefraction is encountered in tropical climates, in trade wind areas, and in most of the principal deserts of the world.

High fields due to ground-based ducts are essentially a fine weather phenomenon. Inland, during fine weather, ducting is most noticeable at night. Over the sea ducting is most marked where the warm dry air of an adjacent land-mass extends out over a comparatively cool sea. Areas of divergence, which favor elevated duct formation, appear to be most persistent over ocean areas from 10° to 40° north and south latitudes, especially during winter months. [Moler and Holden, 1960; Randall, 1964]. Elevated ducts are usually less important than ground-based ducts for tropospheric propagation.

10.2 Climatic Regions

Climatic regions may be defined in several different ways: (1) by geographic areas on a map, (2) by average meteorological conditions, (3) by the predominance of various propagation mechanisms or (4) by averages of available data. In various so-called "climates," at different times of day or seasons of the year, different propagation mechanisms may be dominant. For example, in a continental temperate climate the characteristics of a received signal over a given path may be quite different in the early morning hours in May than during the afternoon hours in February.

Based on our current knowledge of meteorological conditions and their effects on radio propagation, the International Radio Consultative Committee [CCIR 1963f] has defined several "climates." A large amount of data is available from continental temperate and maritime temperate climates. Other climatic regions, where few data are available, are discussed in annex III. The division into radio climates is somewhat arbitrary, based on present knowledge of radio meteorology, and is not necessarily the same as the division into meteorological climates [Haurwitz and Austin, 1944].

World maps of minimum monthly mean N_o, figure 4.1, and of the annual range of monthly mean N_s, figure III.31, may be useful in deciding which climate or climates are applicable in a given region. The boundaries between various climatic regions are not well defined. In some cases it may be necessary to interpolate between the curves for two climates giving additional weight to the one whose occurrence is considered more likely.

Some important characteristics of the climatic regions for which estimates of time variability are shown, are noted below:

1. Continental Temperate characterized by an annual mean N_s of about 320 N-units with an annual range of monthly mean N_s of 20 to 40 N-units. A continental climate in a large land mass shows extremes of temperature in a "temperate" zone, such as 30° to 60° north or south latitude. Pronounced diurnal and seasonal changes in propagation are expected to occur. On the east coast of the United States the annual range of N_s may be as much as 40 to 50 N-units due to contrasting effects of arctic or tropical maritime air masses which may move into the area from the north or from the south.

2. Maritime Temperate Overland characterized by an annual mean N_s of about 320 N-units with a rather small annual range of monthly mean N_s of 20 to 30 N-units. Such climatic regions are usually located from 20° to 50° north or south latitude, near the sea, where prevailing winds, unobstructed by mountains, carry moist maritime air inland. These conditions are typical of the United Kingdom, the west coasts of North America and Europe and the northwestern coastal areas of Africa.

Although the islands of Japan lie within this range of latitude the climate differs in showing a much greater annual range of monthly mean N_s, about 60 N-units, the prevailing winds have traversed a large land mass, and the terrain is rugged. One would therefore not expect to find radio propagation conditions similar to those in the United Kingdom although

the annual mean N_s is 310 to 320 N-units in each location. Climate 1 is probably more appropriate than climate 2 in this area, but ducting may be important in coastal and over-sea areas of Japan as much as 5 percent of the time in summer.

3. Maritime Temperate Oversea coastal and oversea areas with the same general characteristics as those for climate 2. The distinction made is that a radio path with both horizons on the sea is considered to be an oversea path; otherwise climate 2 is used. Ducting is rather common for a small fraction of time between the United Kingdom and the European Continent, and along the west coast of the United States and Mexico.

4. Maritime Subtropical Overland characterized by an annual mean N_s of about 370 N-units with an annual range of monthly mean N_s of 30 to 60 N-units. Such climates may be found from about 10° to 30° north and south latitude, usually on lowlands near the sea with definite rainy and dry seasons. Where the land area is dry radio-ducts may be present for a considerable part of the year.

5. Maritime Subtropical Oversea conditions observed in coastal areas with the same range of latitude as climate 4. The curves for this climate were based on an inadequate amount of data and have been deleted. It is suggested that the curves for climates 3 or 4 be used, selecting whichever seems more applicable to each specific case.

6. Desert, Sahara characterized by an annual mean N_s of about 280 N-units with year-round semiarid conditions. The annual range of monthly mean N_s may be from 20 to 80 N-units.

7. Equatorial a maritime climate with an annual mean N_s of about 360 N-units and annual range of 0 to 30 N-units. Such climates may be observed from 20°N to 20°S latitude and are characterized by monotonous heavy rains and high average summer temperatures. Typical equatorial climates occur along the Ivory Coast and in the Congo of Africa.

8. Continental Subtropical typified by the Sudan and monsoon climates, with an annual mean N_s of about 320 N-units and an annual range of 60 to 100 N-units. This is a hot climate with seasonal extremes of winter drought and summer rainfall, usually located from 20° to 40°N latitude.

A continental polar climate, for which no curves are shown, may also be defined. Temperatures are low to moderate all year round. The annual mean N_s is about 310 N-units with an annual range of monthly mean N_s of 10 to 40 N-units. Under polar conditions, which may occur in middle latitudes as well as in polar regions, radio propagation would be expected to show somewhat less variability than in a continental temperate climate. Long-term median values of transmission loss are expected to agree with the reference values L_{cr}

High mountain areas or plateaus in a continental climate are characterized by low values of N_s and year-round semiarid conditions. The central part of Australia with its hot dry desert climate and an annual range of N_s as much as 50 to 70 N-units may be intermediate between climates 1 and 6.

Prediction of long-term median reference values of transmission loss, by the methods of sections 3 to 9, takes advantage of theory in allowing for the effects of path geometry and radio ray refraction in a standard atmosphere. Meteorological information is used to distinguish between climatic regions. Median values of data available in each of these regions are related to the long-term reference value by means of a parameter $V(0.5, d_e)$ which is a function of an "effective distance," d_e, defined below. Long-term fading about the median for each climatic region is plotted in a series of figures as a function of d_e. For regions where a large amount of data is available, curves are presented that show frequency-related effects. (Seasonal and diurnal changes are given in annex III for a continental temperate climate.)

10.3 The Effective Distance, d_e

Empirical estimates of long-term power fading depend on an effective distance, d_e, which has been found superior to other parameters such as path length, angular distance, distance between actual horizons, or distance between theoretical horizons over a smooth earth. The effective distance makes allowance for effective antenna heights and some allowance for frequency.

Define θ_{s1} as the angular distance where diffraction and forward scatter transmission loss are approximately equal over a smooth earth of effective radius a = 9000 kilometers, and define d_{s1} as $9000\ \theta_{s1}^*$. Then:

$$d_{s1} = 65(100/f)^{\frac{1}{3}} \text{ km.} \tag{10.1}$$

The path length, d, is compared with the sum of d_{s1} and the smooth-earth distances to the radio horizons:

$$d_L = 3\sqrt{2h_{te}} + 3\sqrt{2h_{re}} \text{ km,} \tag{10.2}$$

where the effective antenna heights h_{te} and h_{re} are expressed in meters and the radio frequency f in MHz.

It has been observed that the long-term variability of hourly medians is greatest on the average for values of d only slightly greater than the sum of d_{s1} and d_L. The effective distance d_e is arbitrarily defined as:

for $d \leq d_L + d_{s1}$, $\quad d_e = 130\ d/(d_L + d_{s1})$ km (10.3a)

for $d > d_L + d_{s1}$ $\quad d_e = 130 + d - (d_L + d_{s1})$ km. (10.3b)

10.4 The Functions $V(0.5, d_e)$ and $Y(q, d_e)$

The predicted median long-term transmission loss for a given climatic region $L_n(0.5)$, characterized by a subscript n, is related to the calculated long-term reference value L_{cr} by means of the function $V(0.5, d_e)$

$$L_n(0.5) = L_{cr} - V_n(0.5, d_e) \quad \text{db} \tag{10.4}$$

where $L_n(0.5)$ is the predicted transmission loss exceeded by half of all hourly medians in a given climatic region. $V_n(0.5, d_e)$ is shown on figure 10.13 for several climates as a function of the effective distance d_e. For the special case of forward scatter during winter afternoons in a temperate continental climate, $V(0.5) = 0$ and $L(0.5) = L_{cr}$. In all other cases, the calculated long-term reference value L_{cr} should be adjusted to the median $L_n(0.5)$ for the particular climatic region or time period considered. The function $F(\theta d)$ in the scatter prediction of a long-term reference median contains an empirical adjustment to data. The term $V(0.5, d_e)$ provides a further adjustment to data for all propagation mechanisms and for different climatic regions and periods of time.

In general, the transmission loss not exceeded for a fraction q of hourly medians is

$$L_n(q) = L_n(0.5) - Y_n(q, d_e) \quad \text{db} \tag{10.5}$$

where $Y_n(q, d_e)$ is the variability of $L_n(q)$ relative to its long-term median value $L_n(0.5)$. For a specified climatic region and a given effective distance, the cumulative distribution of transmission loss may be obtained from (10.5). In a continental temperate climate transmission loss is often nearly log-normally distributed. The standard deviation may be as much as twenty decibels for short transhorizon paths where the mechanisms of diffraction and forward scatter are about equally important. When a propagation path in a maritime temperate climate is over water, a log-normal distribution may be expected from $L(0.5)$ to $L(0.999)$, but considerably higher fields are expected for small fractions of time when pronounced superrefraction and ducting are present.

10.5 Continental Temperate Climate

Data from the U.S.A., West Germany, and France provide the basis for predicting long-term power fading in a continental temperate climate. More than half a million hourly median values of basic transmission loss recorded over some two hundred paths were used in developing these estimates.

Figure 10.14 shows basic estimates Y(q, 100 MHz) of variability in a continental temperate climate. Curves are drawn for fractions 0.1 and 0.9 of all hours of the day for summer, winter and all year for a "typical" year. In the northern temperate zone, "summer" extends from May through October and "winter" from November through April.

A "frequency factor" g(q, f) shown in figure 10.15 adjusts the predicted variability to allow for frequency-related effects:

$$Y(q) = Y(q, d_e, 100 \text{ MHz})\ g(q, f). \qquad (10.6)$$

The function g(q, f) shows a marked increase in variability as frequency is increased above 100 MHz to a maximum at 400 to 500 MHz. Variability then decreases until values at 1 or 2 GHz are similar to those expected at 100 MHz. The empirical curves g(q, f) should not be regarded as an estimate of the dependence of long-term variability on frequency, but represent only an average of many effects, some of which are frequency-sensitive. The apparent frequency dependence is a function of the relative dominance of various propagation mechanisms, and this in turn depends on climate, time of day, season, and the particular types of terrain profiles for which data are available. For example, a heavily forested low altitude path will usually show greater variability than that observed over a treeless high altitude prairie, and this effect is frequency sensitive. An allowance for the year-to-year variability is also included in g(q, f). Data summarized by Williamson et al.[1960] show that L(0.5) varies more from year to year than Y(q). Assuming a normal distribution of L within each year and of L(0.5) from year to year, L would be normally distributed with a median equal to L(0.5) for a "typical" year. Y(q) is then increased by a constant factor, which has been included in g(q, f).

Estimates of Y(0.1) and Y(0.9) are obtained from figures 10.14, 10.15 and from equation 10.6. These estimates are used to obtain a predicted cumulative distribution using the following ratios:

Y(0.0001) = 3.33 Y(0.1)	Y(0.9999) = 2.90 Y(0.9)	
Y(0.001) = 2.73 Y(0.1)	Y(0.999) = 2.41 Y(0.9)	(10.7)
Y(0.01) = 2.00 Y(0.1)	Y(0.99) = 1.82 Y(0.9)	

For example, assume f = 100 MHz, d_e = 112 km, and a predicted reference median basic transmission loss, L_{bcr} = 179 db, so that V(0.5, d_e) = 0.9 db, (figure 10.13), Y(0.1, d_e, 100 MHz) = 8.1 db, and Y(0.9, d_e, 100 MHz) = -5.8 db, (figure 10.14), g(0.1, f) = g(0.9, f) = 1.05 (figure 10.15). Then Y(0.1) = 1.05 Y(0.1, d_e, 100 MHz) = 8.5 db, and Y(0.9) = 1.05 Y(0.9, d_e, 100 MHz) = -6.1 db. Using the ratios given above:

$Y(0.0001) = 28.3$, $Y(0.001) = 23.2$, $Y(0.01) = 8.5$,

$Y(0.9999) = -17.7$, $Y(0.999) = -14.7$, $Y(0.99) = -11.1$, $Y(0.9) = -6.1$.

The median value is

$$L_b(0.5) = L_{bcr} - V(0.5) = 178.1 \quad \text{db}$$

and the predicted distribution of basic transmission loss is;

$L(0.0001) = 149.8$, $L(0.001) = 154.9$, $L(0.01) = 161.1$, $L(0.1) = 169.6$, $L(0.5) = 178.1$, $L(0.9) = 184.2$, $L(0.99) = 189.2$, $L(0.999) = 192.8$ and $L(0.9999) = 195.8$ db.

These values are plotted as a function of time availability, q, on figure 10.16 and show a complete predicted cumulative distribution of basic transmission loss.

For antennas elevated above the horizon, as in ground-to-air or earth-to-space communication, less variability is expected. This is allowed for by a factor $f(\theta_h)$ discussed in annex III. For transhorizon paths $f(\theta_h)$ is unity and does not affect the distribution. For line-of-sight paths $f(\theta_h)$ is nearly unity unless the angle of elevation exceeds 0.15 radians.

Allowance must sometimes be made for other sources of power fading such as attenuation due to rainfall or interference due to reflections from aircraft that may not be adequately represented in available data. For example, at microwave frequencies the distribution of water vapor, oxygen, rain, snow, clouds and fog is important in predicting long-term power fading. Let Y_1, Y_2 - - - Y_n represent estimates corresponding to each of these sources of variability, and let ρ_{ij} be the correlation between variations due to sources i and j. Then the total variability is approximated as:

$$Y^2(q) = \sum_{i+1}^{m} Y_i^2(q) + 2 \sum_{\substack{i,\, j+1 \\ i<j}}^{m} Y_i Y_j \rho_{ij} \qquad (10.8)$$

where $Y(q)$ is positive for $q < 0.5$, zero for $q = 0.5$, and negative for $q > 0.5$. Section 3 shows how to estimate $Y_a(q)$ and $Y_r(q)$ for atmospheric absorption by oxygen and water vapor, and for rain absorption respectively. Let ρ_{1a} be the correlation between variations Y of available data and variations Y_a due to microwave absorption by oxygen and water vapor. Let ρ_{1r} be the correlation between Y and Y_r. Assuming that $\rho_{1a} = 1$, $\rho_{1r} = 0.5$, and $\rho_{ar} = 0$,

$$Y^2(q) = (Y + Y_a)^2 + Y_r^2 + Y\, Y_r \qquad (10.9)$$

This method was used to allow for the effects of rainfall at frequencies above 5 GHz for fractions 0.99 and 0.9999 of all hours in figures I.6 to I.11 of annex I.

Figures 10.17 to 10.22 show variability, Y(q) about the long-term median value as a function of d_e for period of record data in the following frequency groups; 40-88, 88-108, 108-250, 250-450, 450-1000, and > 1000 MHz. The curves on the figures show predicted values of Y(q) for all hours of the year at the median frequency in each group. These medians are: 47.1, 98.7, 192.8, 417, 700, and 1500 MHz for data recorded in a continental temperate climate. Equation (10.6) and figures 10.14 and 10.15 were used to obtain the curves in figures 10.17 to 10.22.

An analytic function fitted to the curves of $V(0.5, d_e)$ and $Y(q, d_e, 100\ MHz)$ is given in annex III. Diurnal and seasonal variations are also discussed and functions listed to predict variability for several times of day and seasons.

10.6 Maritime Temperate Climate

Studies made in the United Kingdom have shown appreciable differences between propagation over land and over sea, particularly at higher frequencies. Data from maritime temperate regions were therefore classified as overland and oversea, where oversea paths are categorized as having the coastal boundaries within their radio horizons. Paths that extend over a mixture of land and sea are included with the overland paths.

The data were divided into frequency groups as follows:

Bands I and II	(40-100 MHz)
Band III	(150-250 MHz)
Bands IV and V	(450-1000 MHz)

Long-term variability of the data for each path about its long-term median value is shown as a function of effective distance in figures 10.23 to 10.28. Curves were drawn through medians of data for each fraction of time q = 0.0001, 0.001, 0.01, 0.1, 0.9, 0.99, 0.999, 0.9999. Figures 10.23 to 10.28 show that it is not practical to use a formula like (10.6) for the maritime temperate climate, because the frequency factor g(q, f) is <u>not</u> independent of d_e, as it is in the case of the continental temperate climate. The importance of tropospheric ducting in a maritime climate is mainly responsible for this difference.

These figures demonstrate greater variability oversea than overland in all frequency groups. The very high fields noted at UHF for small fractions of time are due to persistent layers and ducts that guide the radio energy. In cases of propagation for great distances over water the fields approach free space values for small fractions of time. Curves have been drawn for those distance ranges where data permitted reasonable estimates. Each curve is solid where it is well supported by data, and is dashed for the remainder of its length.

10.7 Other Climates

A limited amount of data available from other climatic regions has been studied, [CCIR 1963f]. Curves showing predicted variability in several climatic regions are shown in annex III, figures III.25 to III.29.

At times it may be necessary to predict radio performance in an area where few if any measurements have been made. In such a case, estimates of variability are based on whatever is known about the meteorological conditions in the area, and their effects on radio propagation, together with results of studies in other climatic regions. If a small amount of radio data is available, this may be compared with predicted cumulative distributions of transmission loss corresponding to somewhat similar meteorological conditions. In this way estimates for relatively unknown areas may be extrapolated from what is known.

10.8 Variability for Knife-Edge Diffraction Paths

The variability of hourly medians for knife-edge diffraction paths can be estimated by considering the path as consisting of two line-of-sight paths in tandem. The diffracting knife-edge then constitutes a common terminal for both line-of-sight paths. The variability of hourly median transmission loss for each of the paths is computed by the methods of this section and characterized by the variability functions

$$V_1(q) = V_1(0.5) + Y_1(q) \quad \text{db}$$

$$V_2(q) = V_2(0.5) + Y_2(q) \quad \text{db}$$

During any particular hour, the total variability function V for the diffraction path would be expected to be the sum of V_1 plus V_2. To obtain the cumulative distribution of all values of V applicable to the total path a convolution of the individual variables V_1 and V_2 may be employed [Davenport and Root, 1958].

Assuming that V_1 and V_2 are statistically independent variables, their convolution is the cumulative distribution of the variable $V = V_1 + V_2$. The cumulative distribution of V may be obtained by selecting n equally-spaced values from the individual distributions of $V_1(q)$ and $V_2(q)$, calculating all possible sums $V_k = V_{1i} + V_{2j}$ and forming the cumulative distribution of all values V_k obtained in this manner.

Another method of convolution that gives good results requires the calculation and ordering of only n, instead of n^2, values of V. As before $V_1(q)$ and $V_2(q)$ are obtained for n equally spaced percentages. Then one set is randomly ordered compared to the other so that the n sums $V = V_1 + V_2$ are randomly ordered. The cumulative distribution of these sums then provides the desired convolution of V_1 and V_2. If the distribution of $V_1 - V_2$ is desired this is the convolution of V_1 and $-V_2$.

Computations required to estimate long-term variability over a knife-edge diffraction path are given in the example described in section 7.5.

Percent of Time Trapping Frequency is Less Than 3000 MHz: **February**

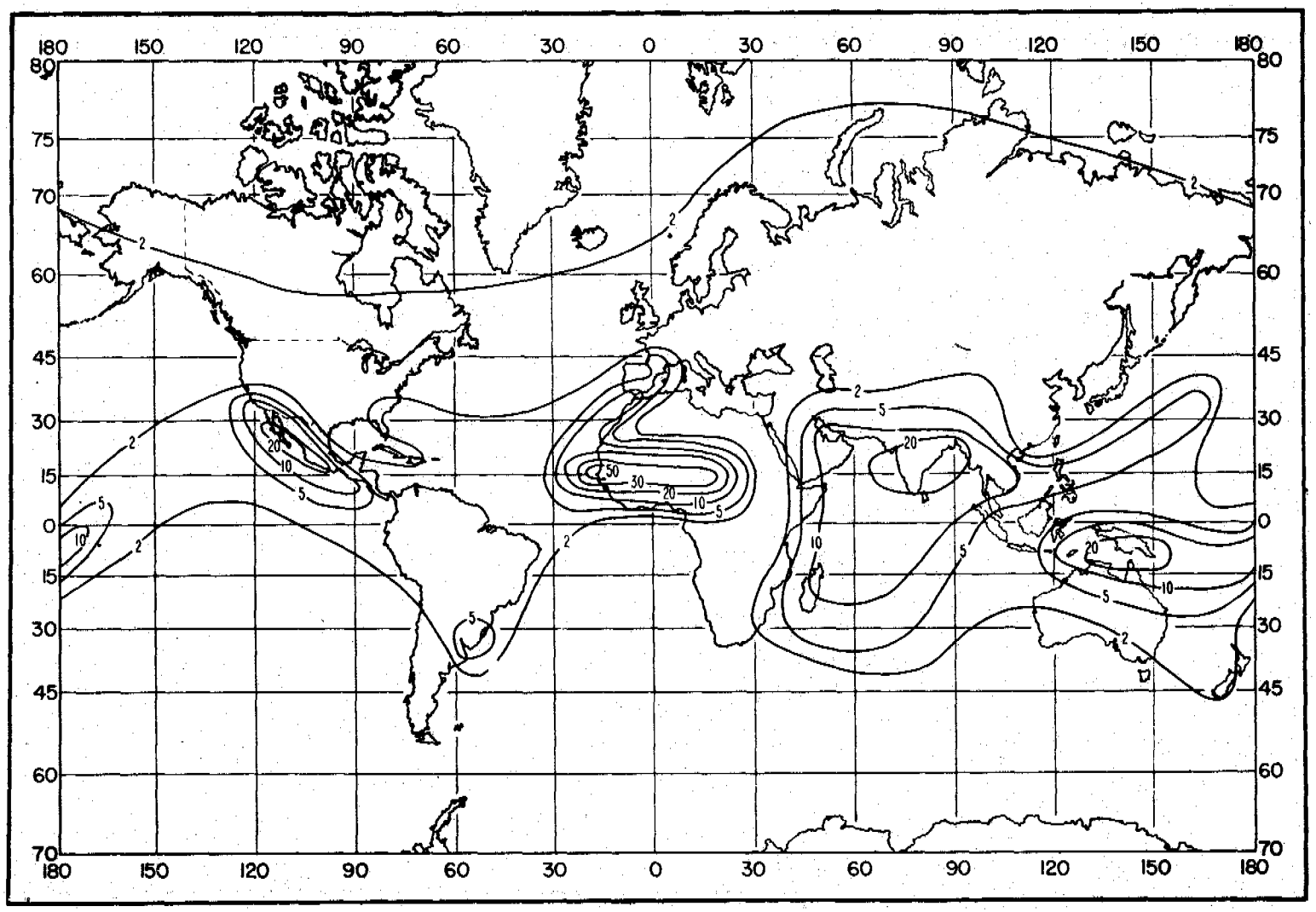

Figure 10.1

Percent of Time Trapping Frequency is Less Than 3000 MHz: May

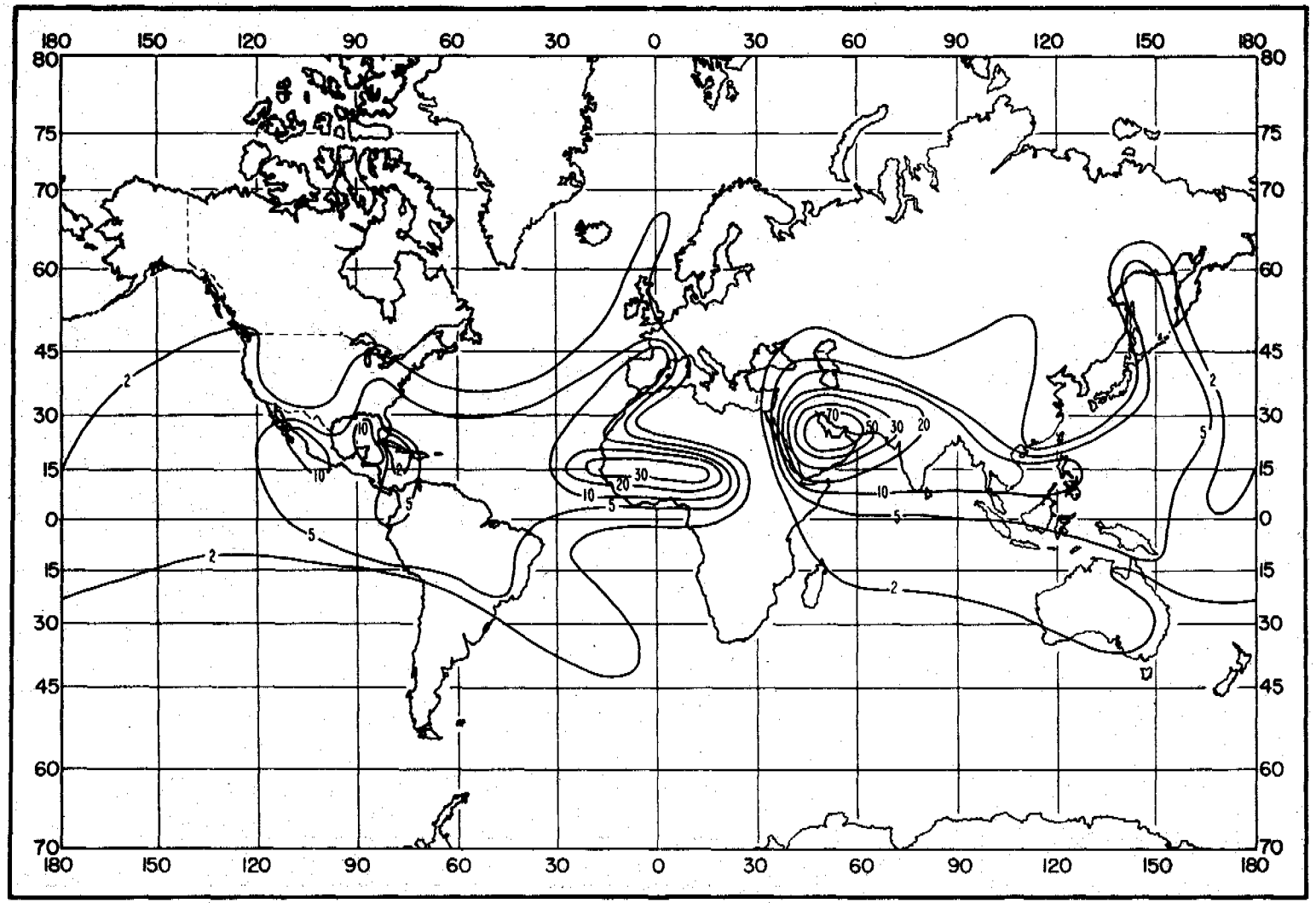

Figure 10.2

Percent of Time Trapping Frequency is Less Than 3000 MHz: August

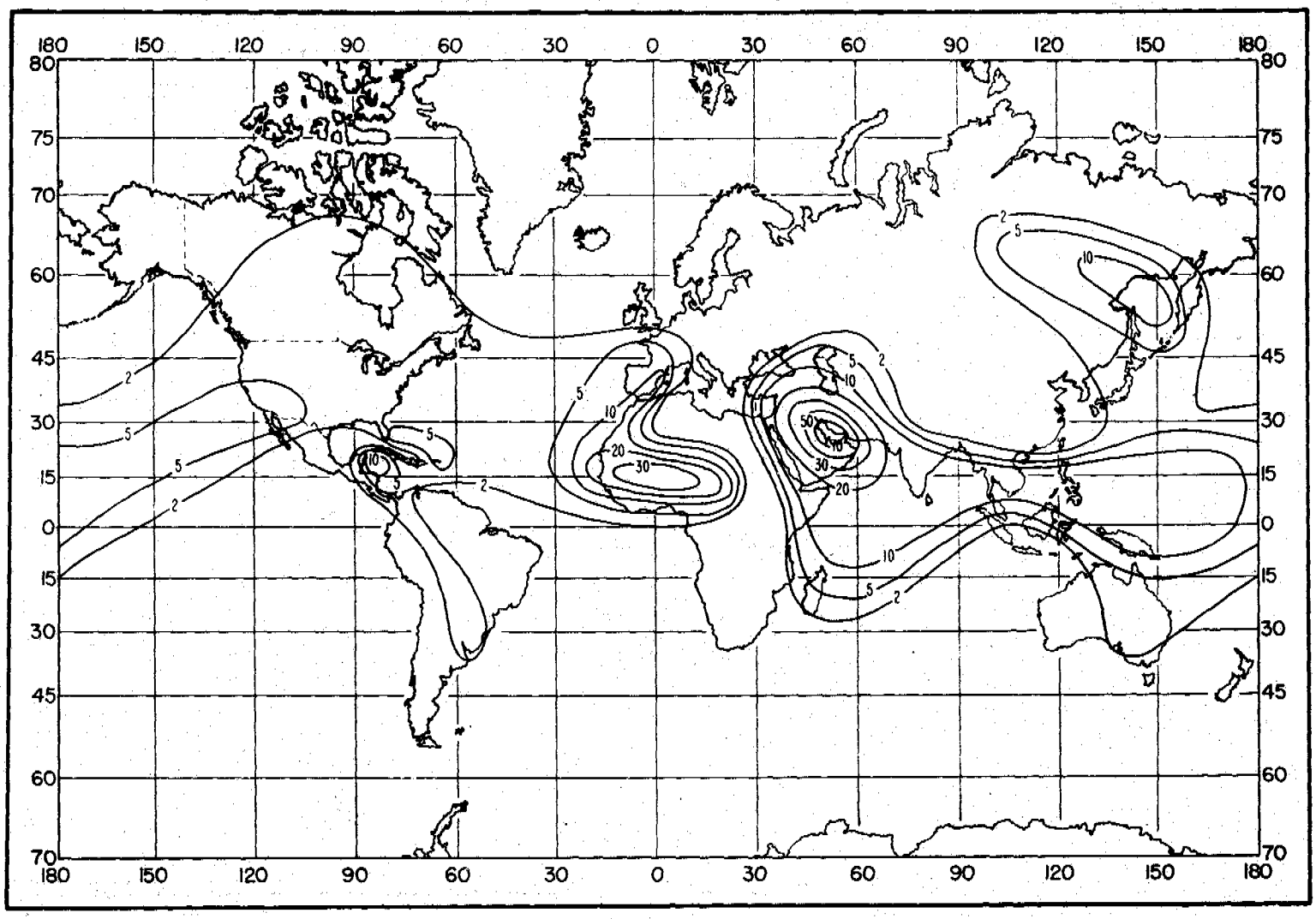

Figure 10.3

Percent of Time Trapping Frequency is Less Than 3000 MHz: November

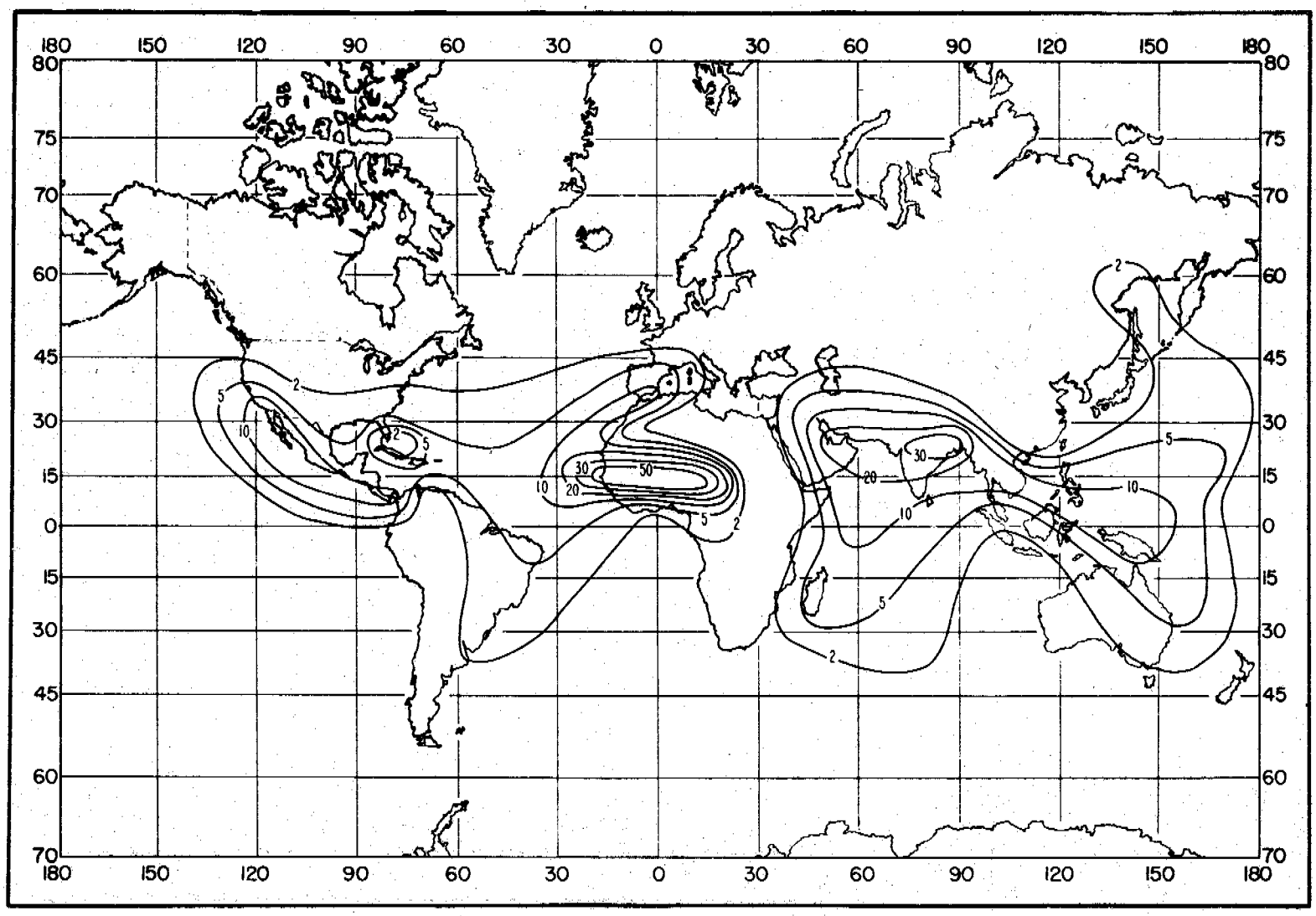

Figure 10.4

Percent of Time Trapping Frequency is Less Than 1000 MHz: February

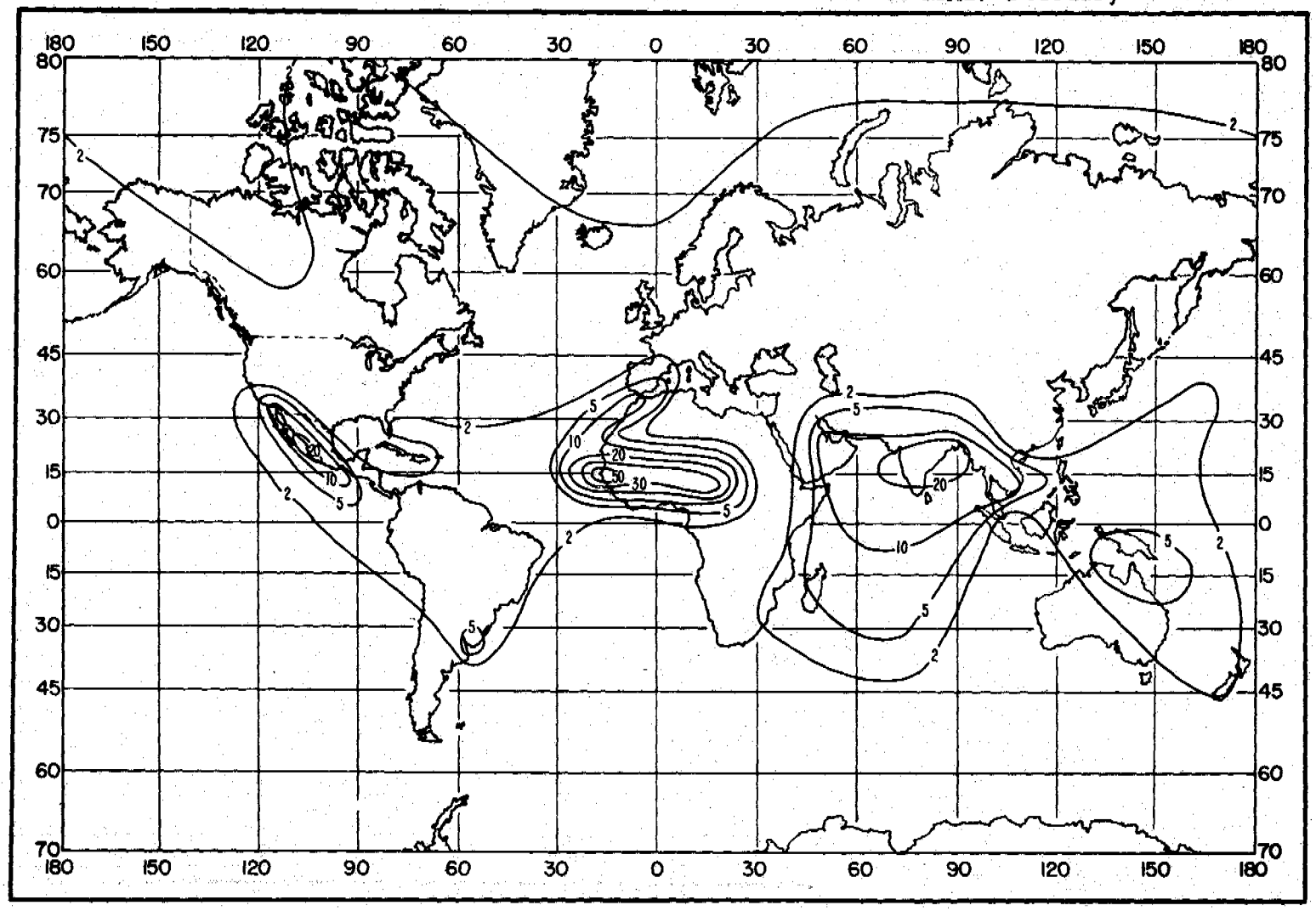

Figure 10.5

Percent of Time Trapping Frequency is Less Than 1000 MHz: May

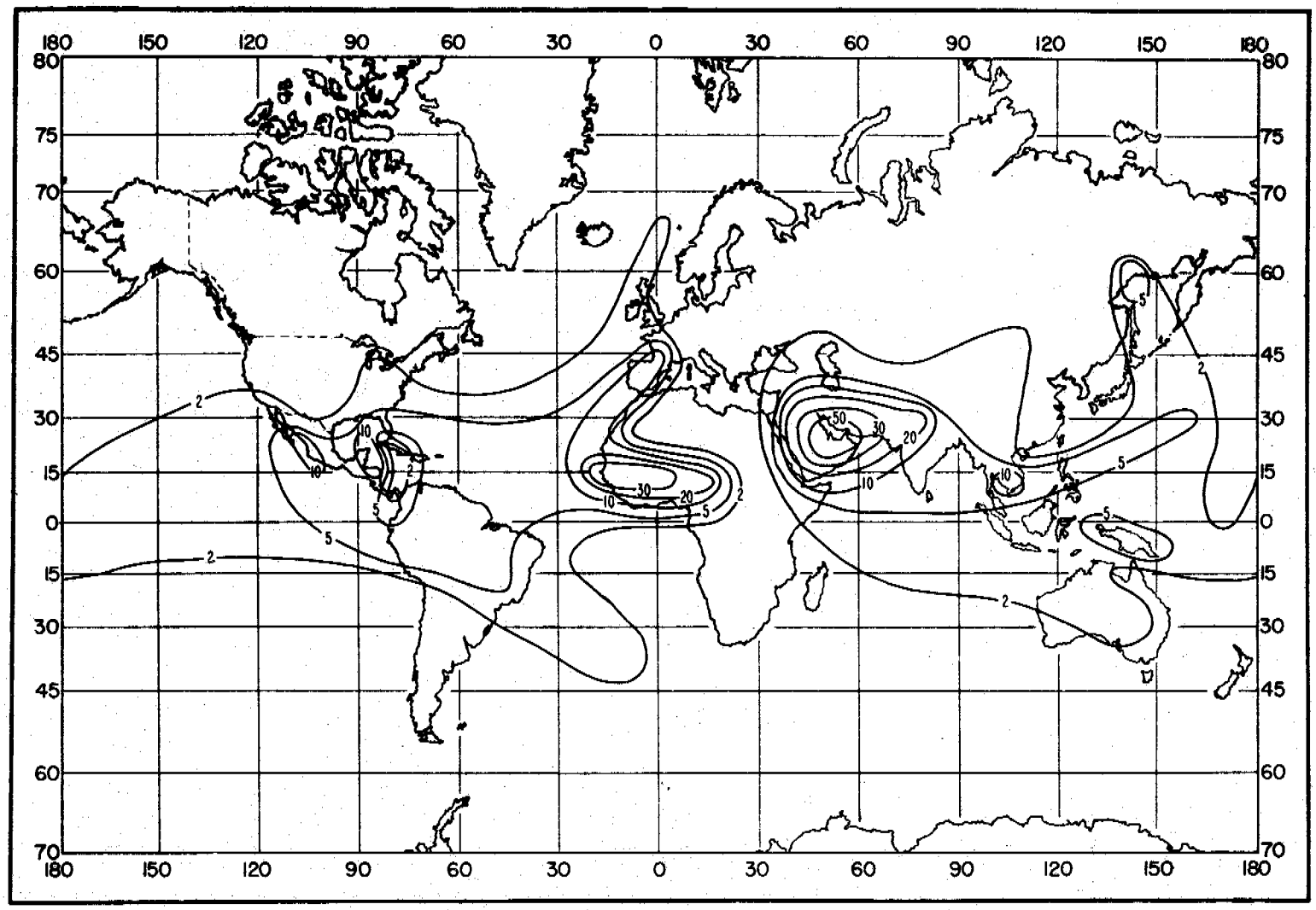

Figure 10.6

Percent of Time Trapping Frequency is Less Than 1000 MHz: August

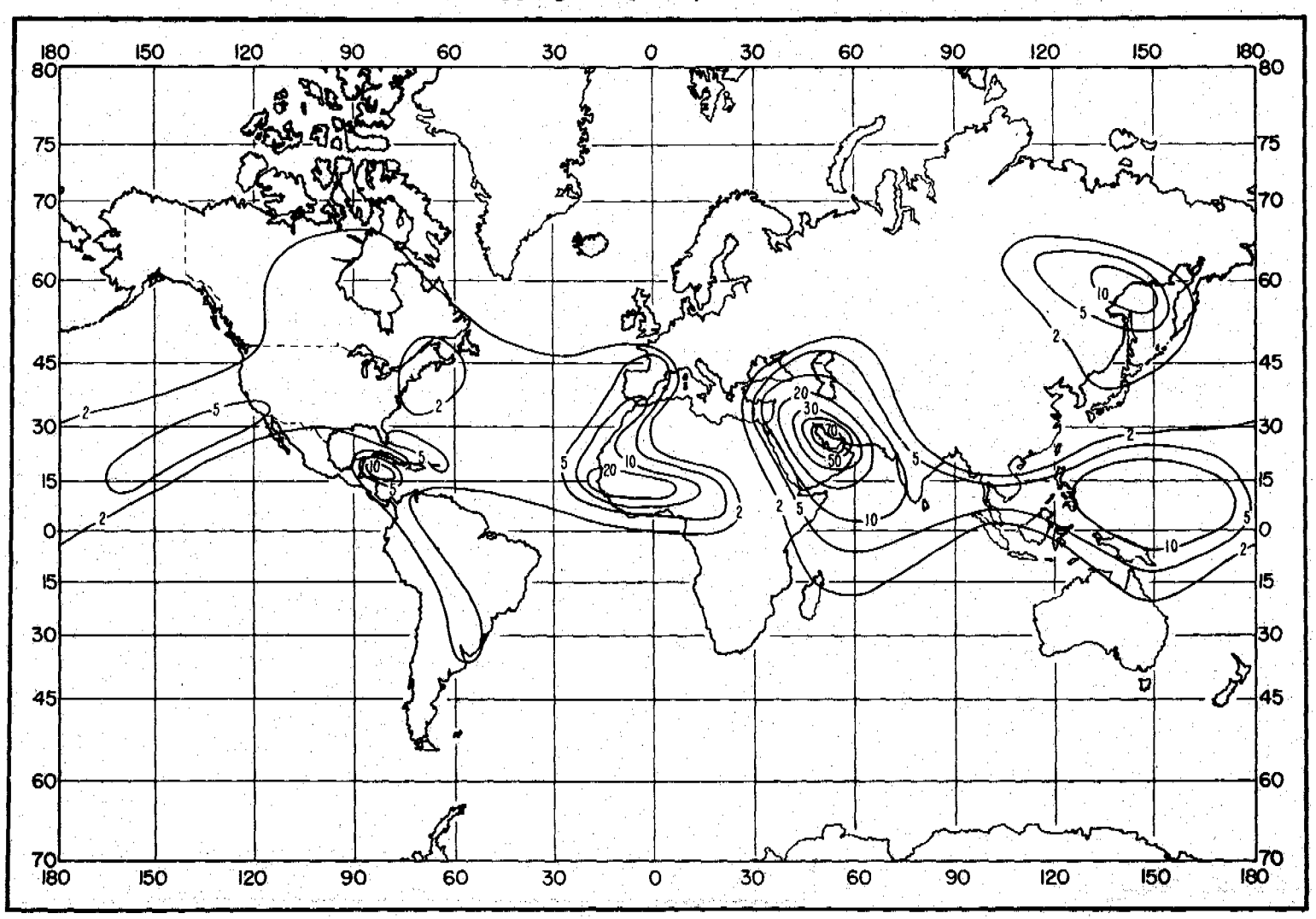

Figure 10.7

Percent of Time Trapping Frequency is Less Than 1000 MHz: November

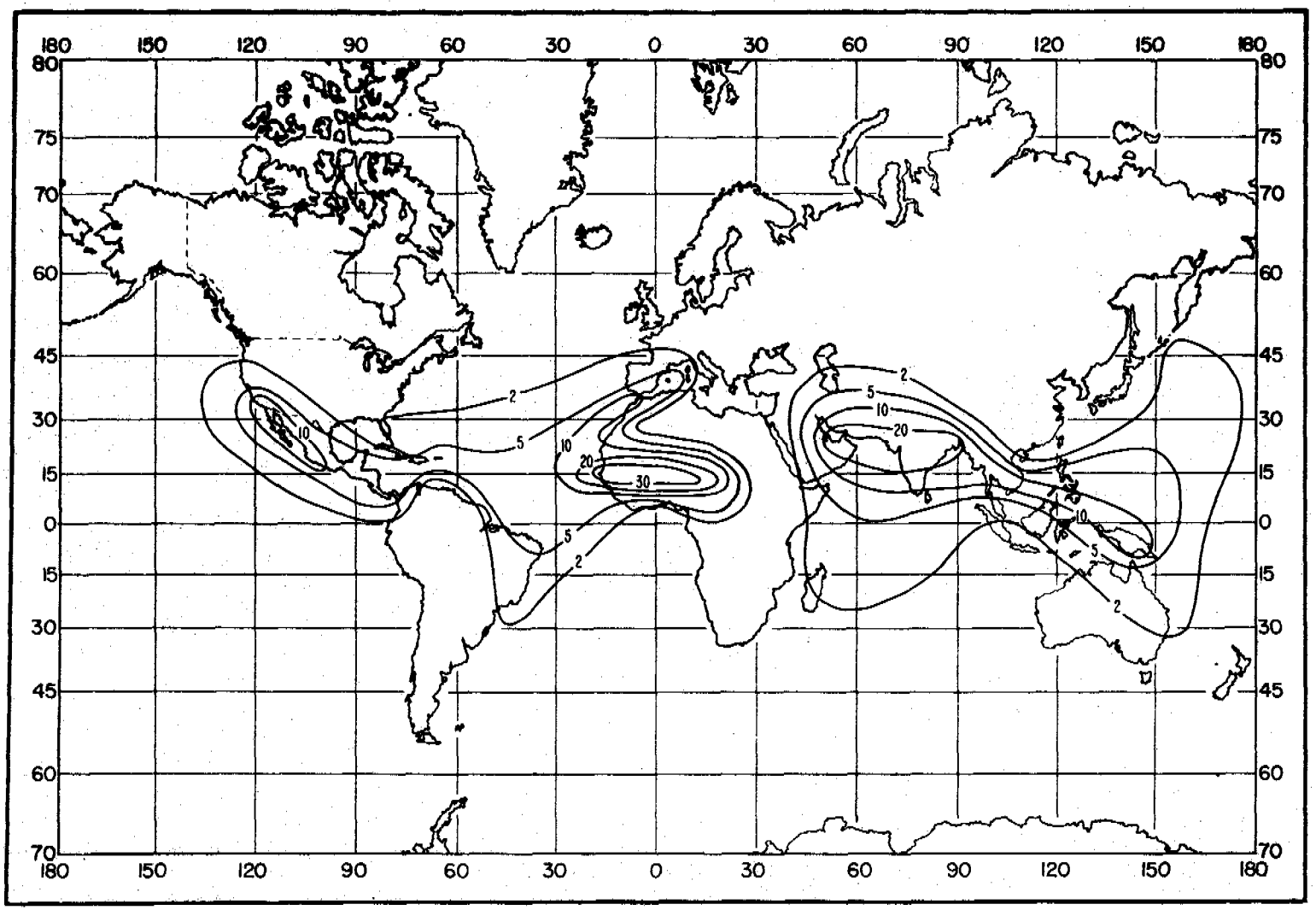

Figure 10.8

Percent of Time Trapping Frequency is Less Than 300 MHz: February

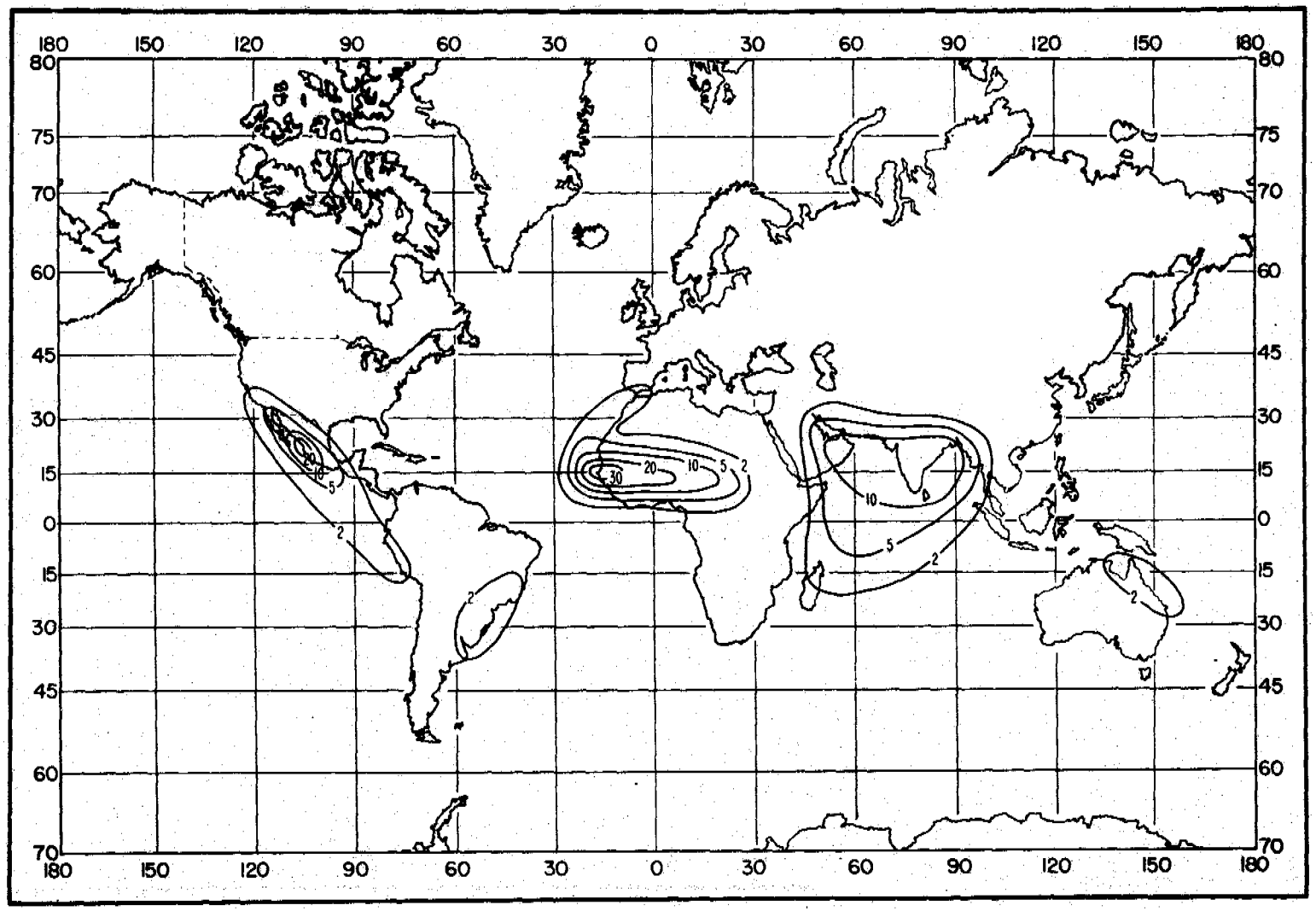

Figure 10.9

Percent of Time Trapping Frequency is Less Than 300 MHz: May

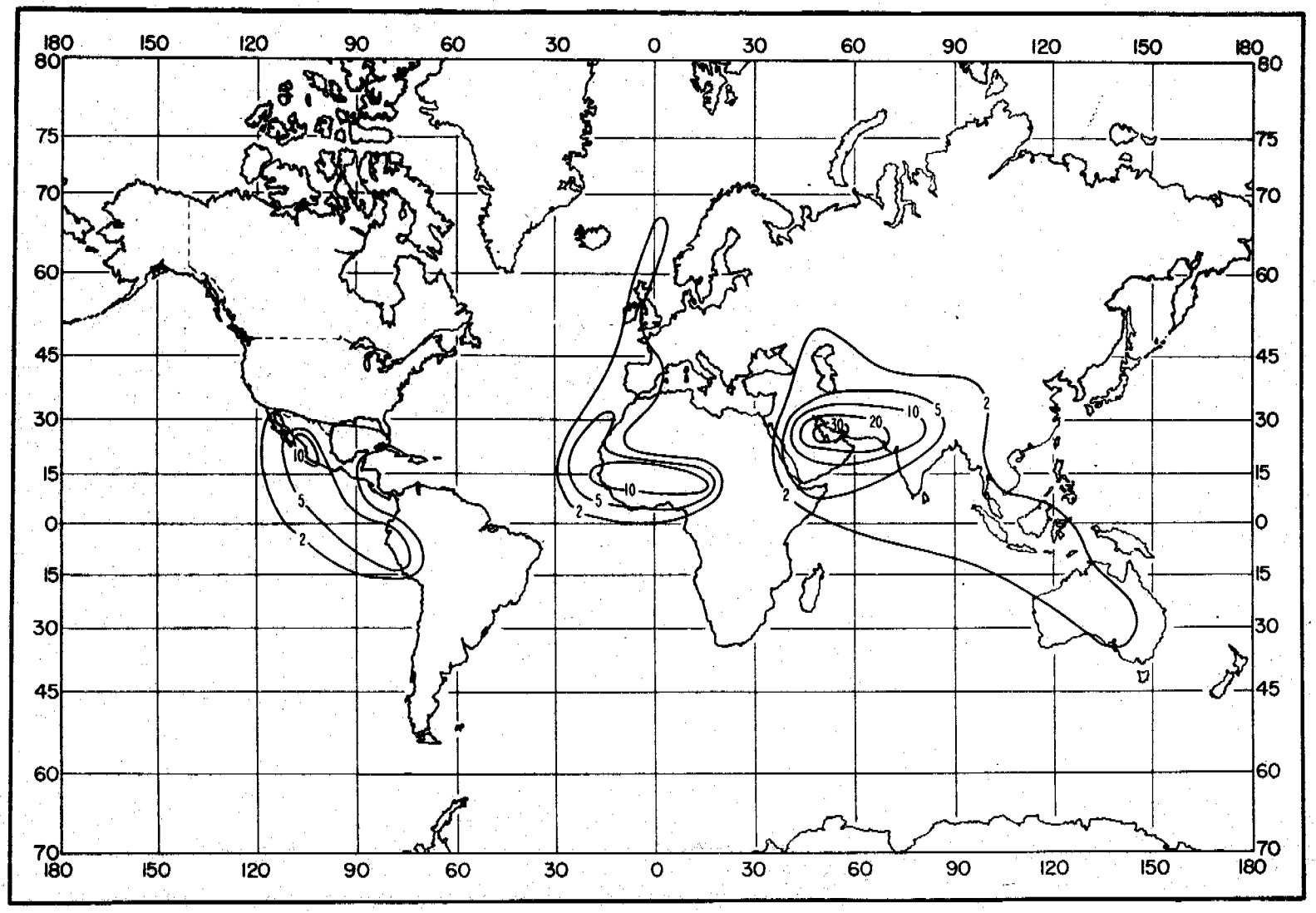

Figure 10.10

Percent of Time Trapping Frequency is Less Than 300 MHz: August

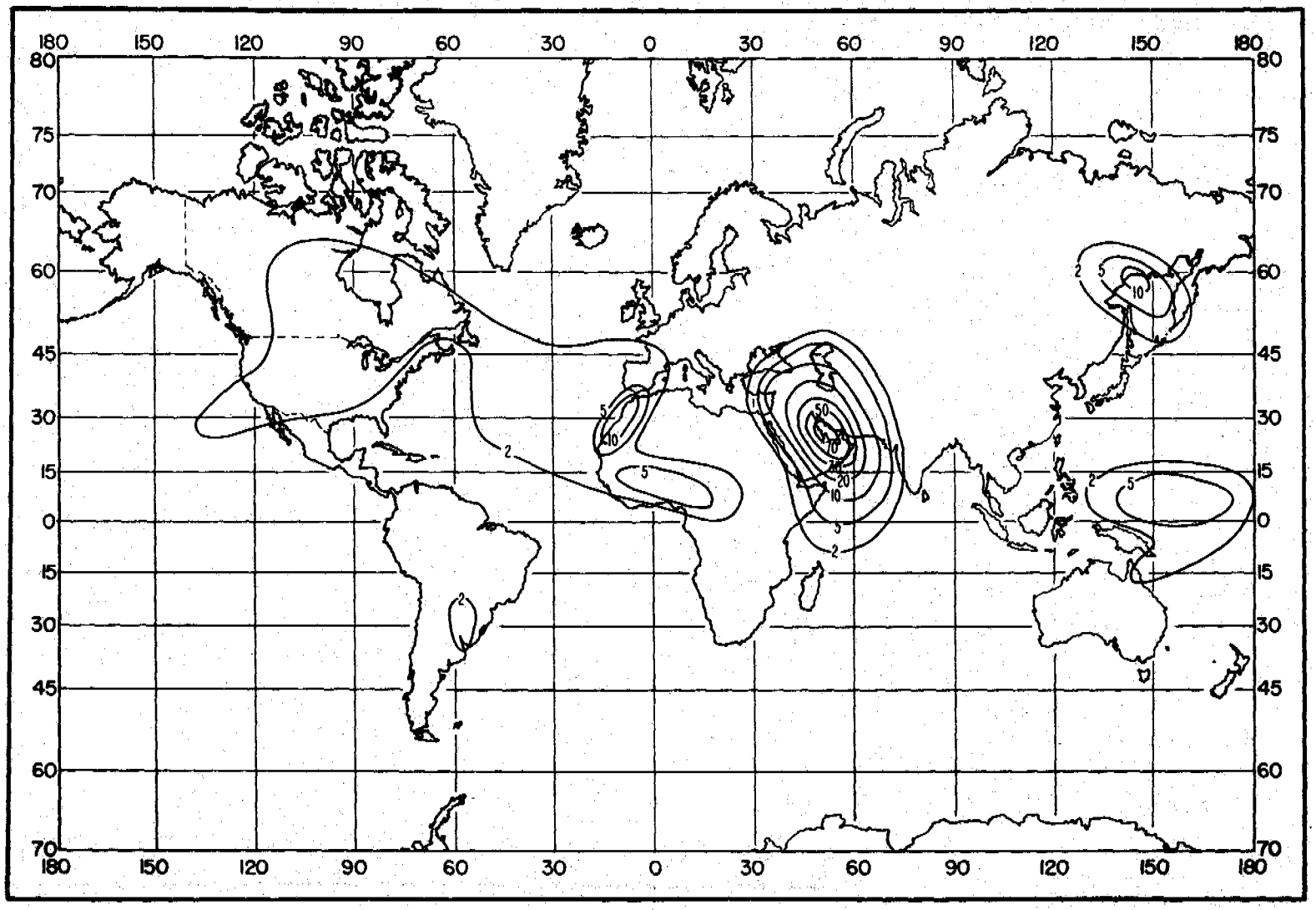

Figure 10.11

Percent of Time Trapping Frequency is Less Than 300 MHz: November

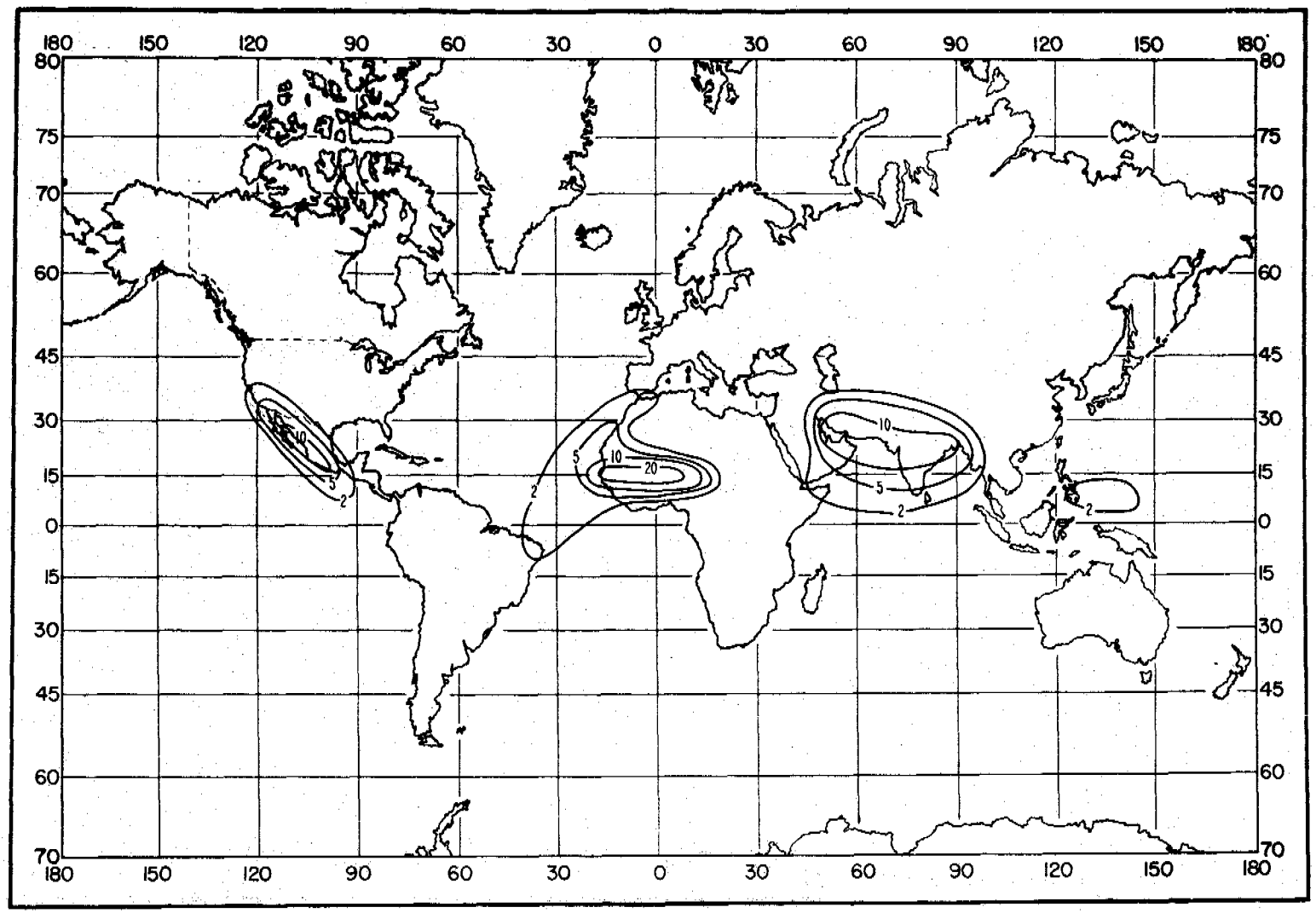

Figure 10.12

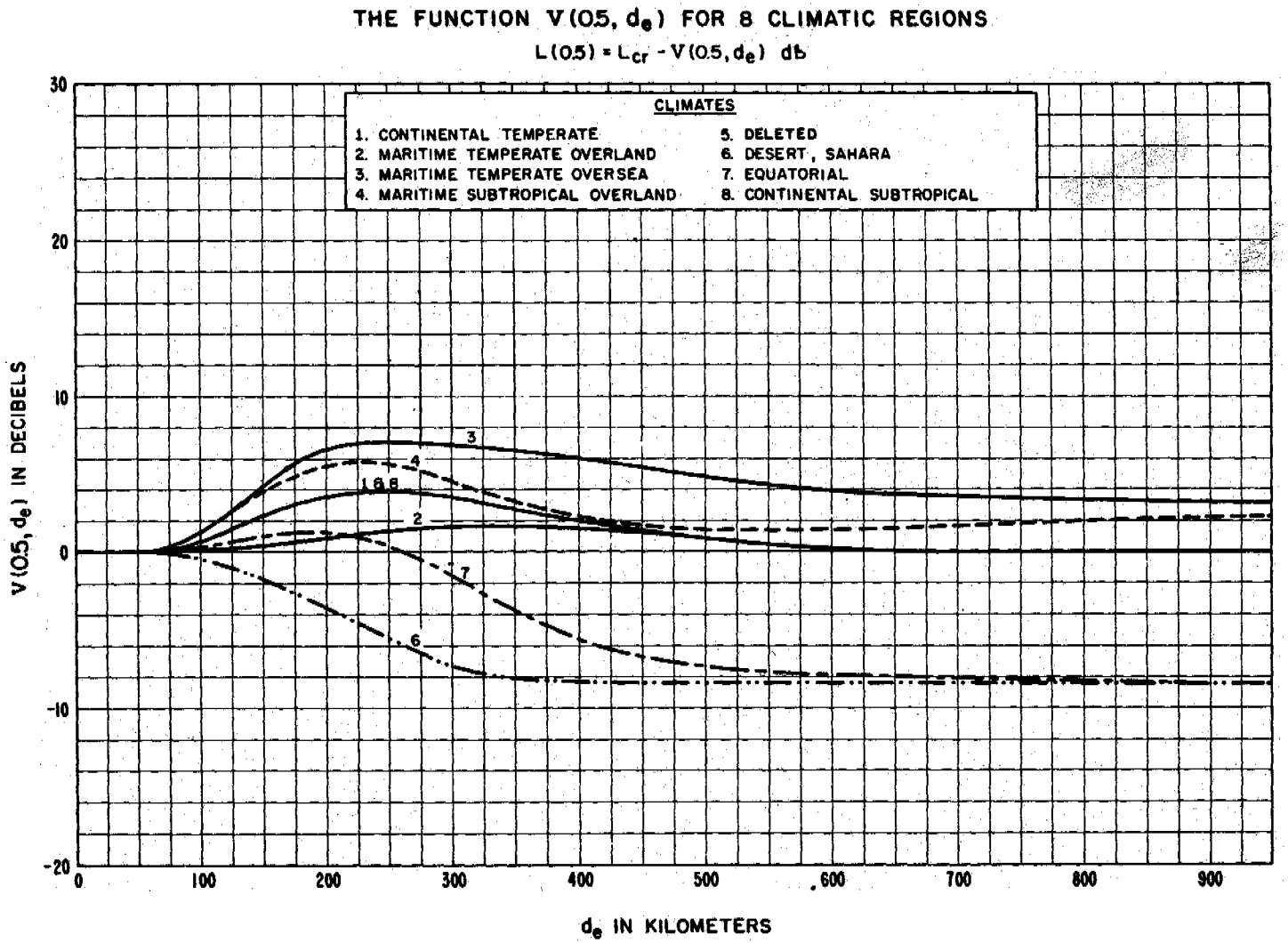
THE FUNCTION V(0.5, d_e) FOR 8 CLIMATIC REGIONS
L(0.5) = L_{cr} - V(0.5, d_e) db
CLIMATES
1. CONTINENTAL TEMPERATE
2. MARITIME TEMPERATE OVERLAND
3. MARITIME TEMPERATE OVERSEA
4. MARITIME SUBTROPICAL OVERLAND
5. DELETED
6. DESERT, SAHARA
7. EQUATORIAL
8. CONTINENTAL SUBTROPICAL
V(0.5, d_e) IN DECIBELS
30
20
10
0
-10
-20
0
100
200
300
400
500
600
700
800
900
d_e IN KILOMETERS
3
4
1 & 8
2
7
6

Figure 10.13

LONG-TERM POWER FADING FUNCTION $Y(q, d_e, 100\ MHz)$

CONTINENTAL TEMPERATE CLIMATE

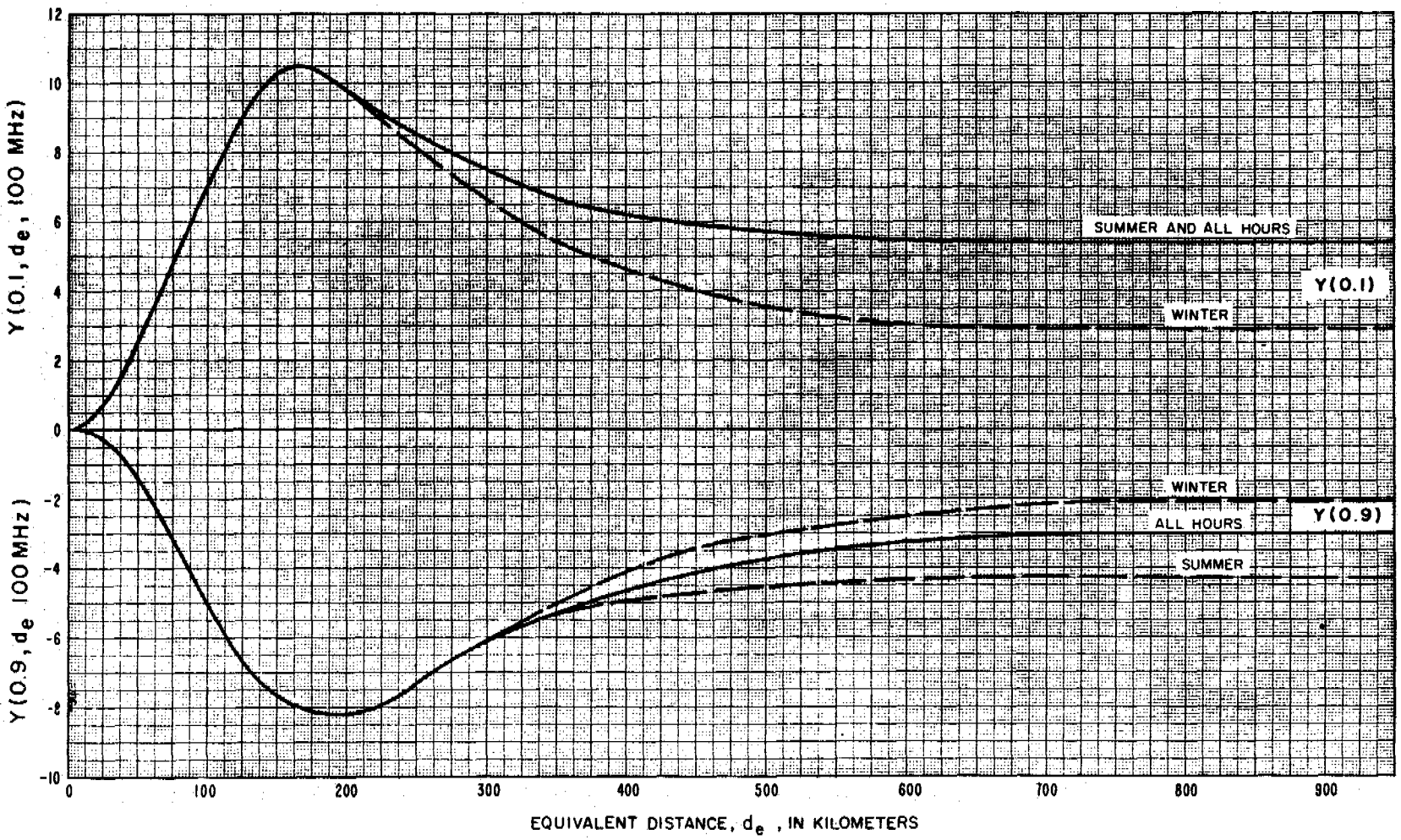

Figure 10.14

POWER FADING ADJUSTMENT FACTOR g(q,f)

BASED ON U.S. OVERLAND DATA

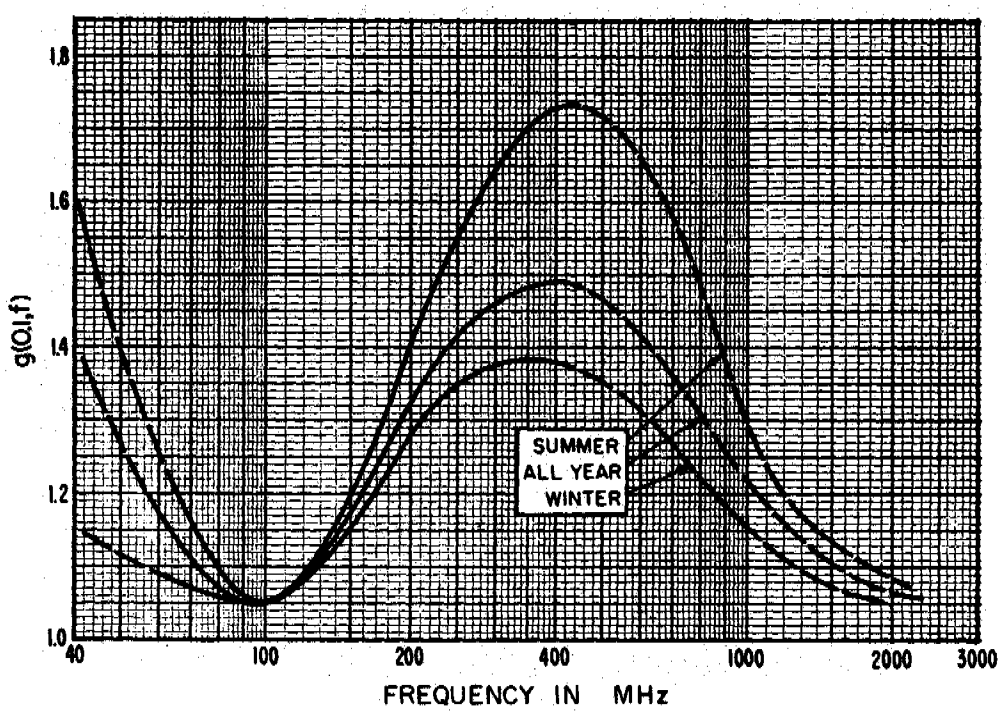

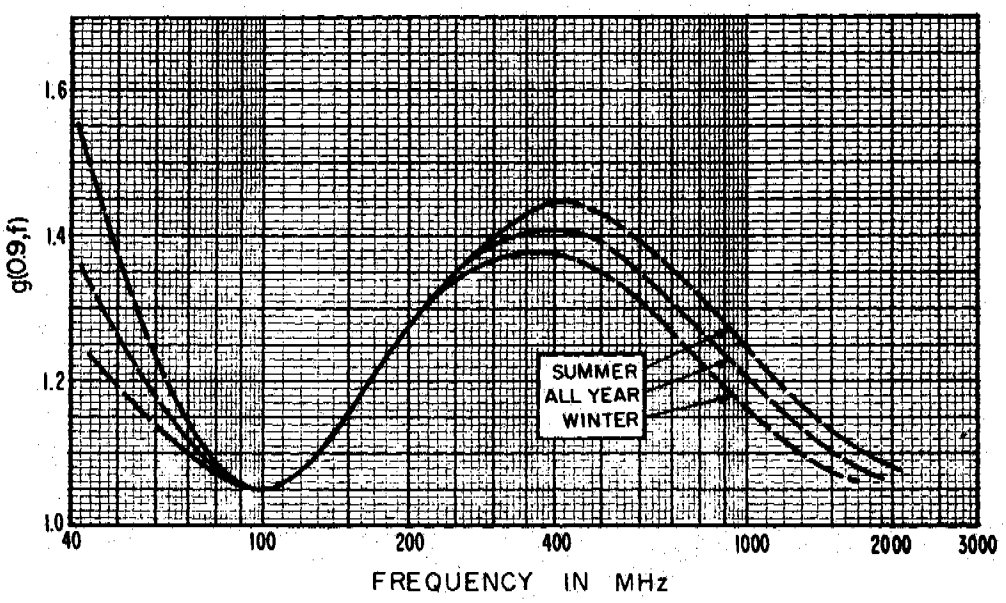

Figure 10.15

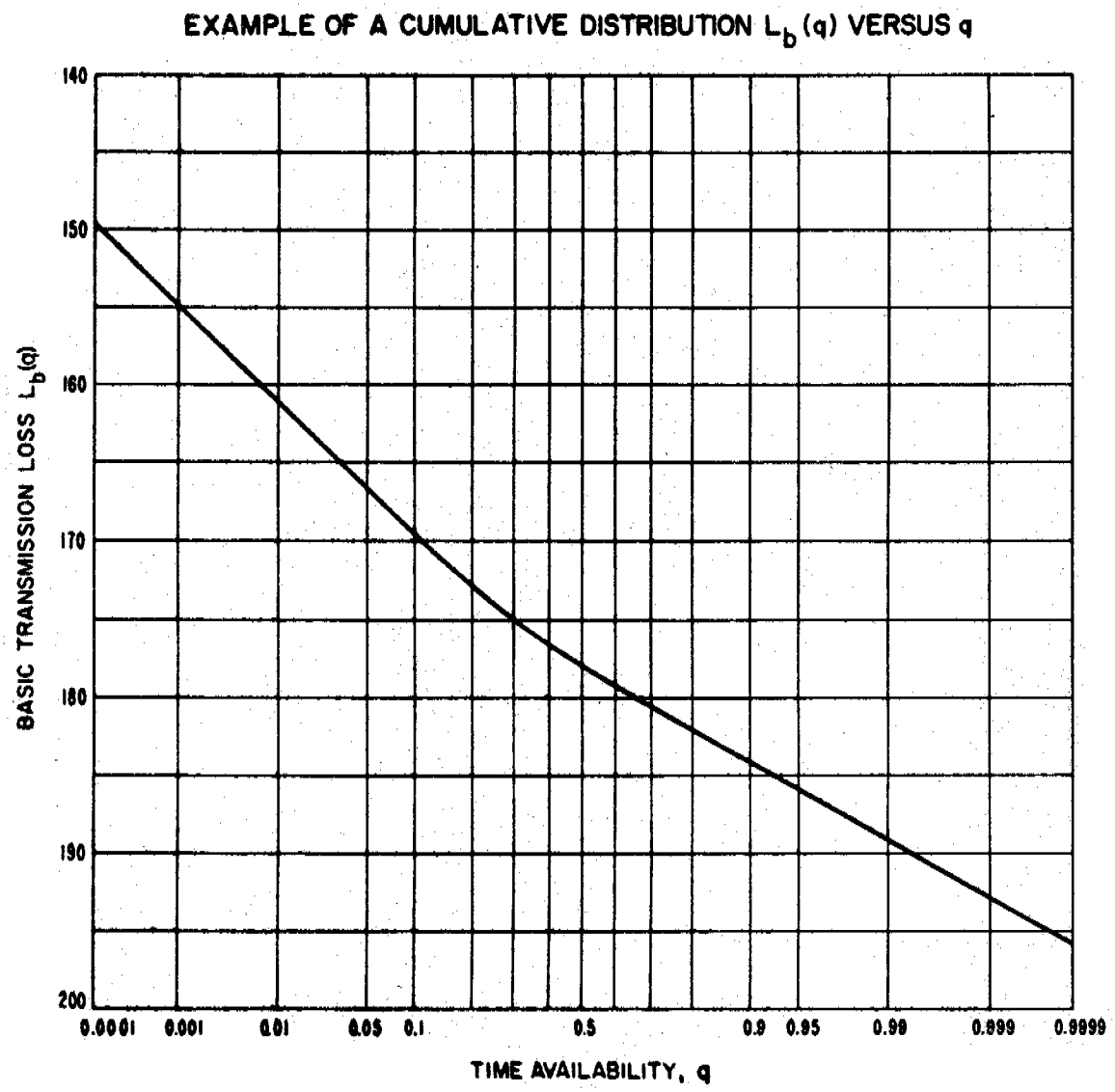
EXAMPLE OF A CUMULATIVE DISTRIBUTION $L_b(q)$ VERSUS q
BASIC TRANSMISSION LOSS $L_b(q)$
140
150
160
170
180
190
200
0.0001
0.001
0.01
0.05
0.1
0.5
0.9
0.95
0.99
0.999
0.9999
TIME AVAILABILITY, q

Figure 10.16

LONG-TERM POWER FADING
CONTINENTAL TEMPERATE CLIMATE, 40 - 88 MHz

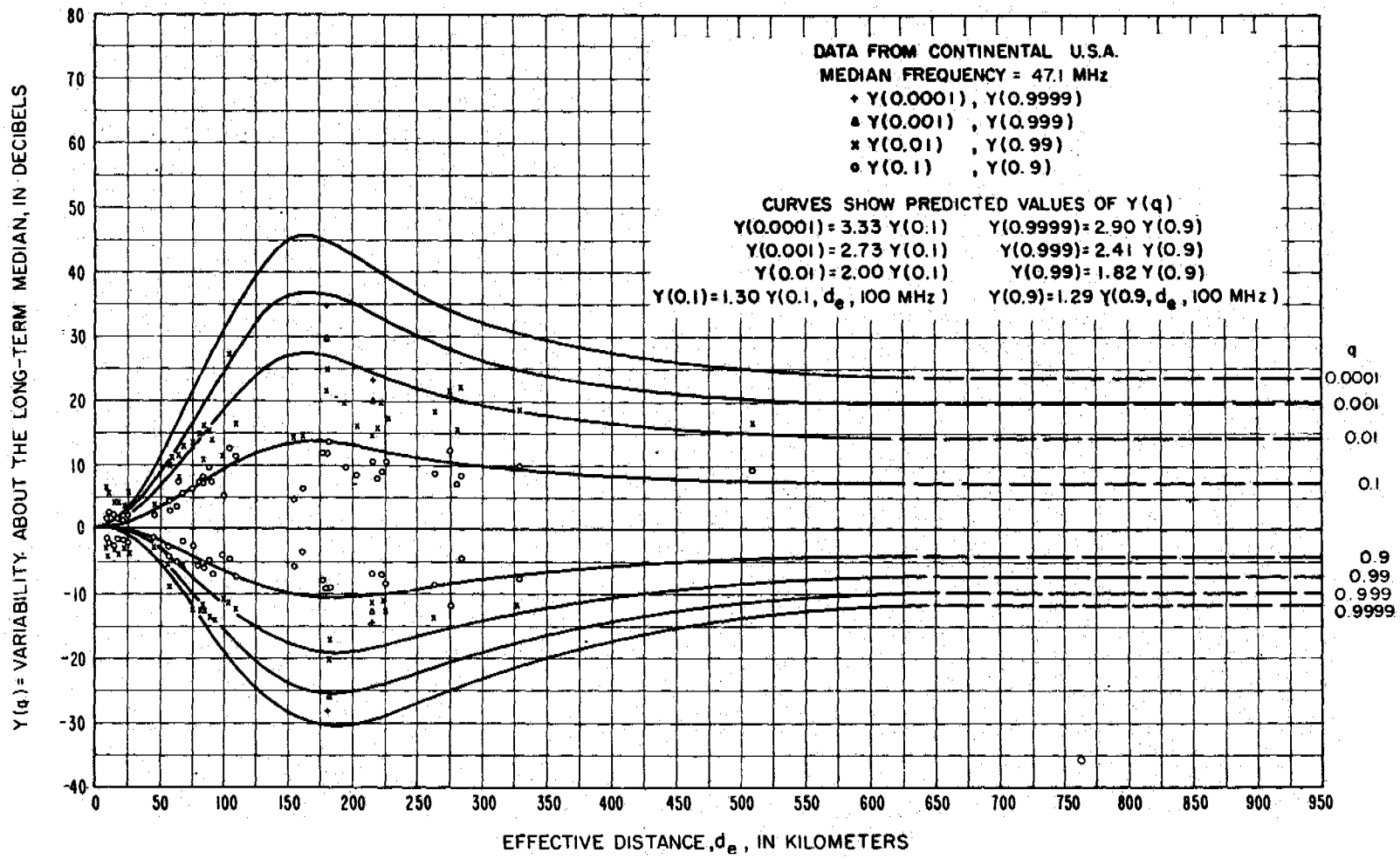

Figure 10.17

LONG-TERM POWER FADING
CONTINENTAL TEMPERATE CLIMATE, 88-108 MHz

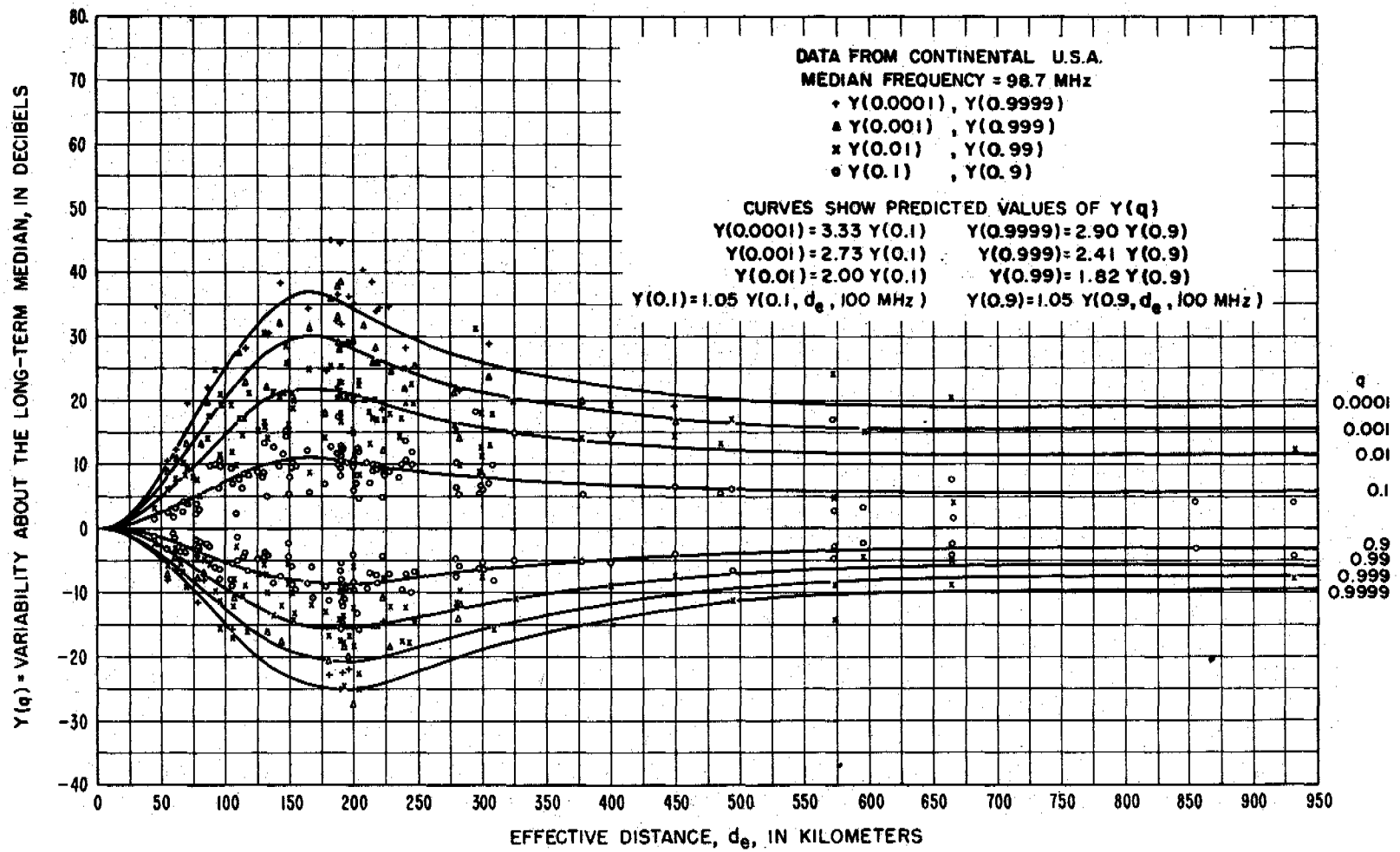

Figure 10.18

LONG-TERM POWER FADING
CONTINENTAL TEMPERATE CLIMATE, 108-250 MHz

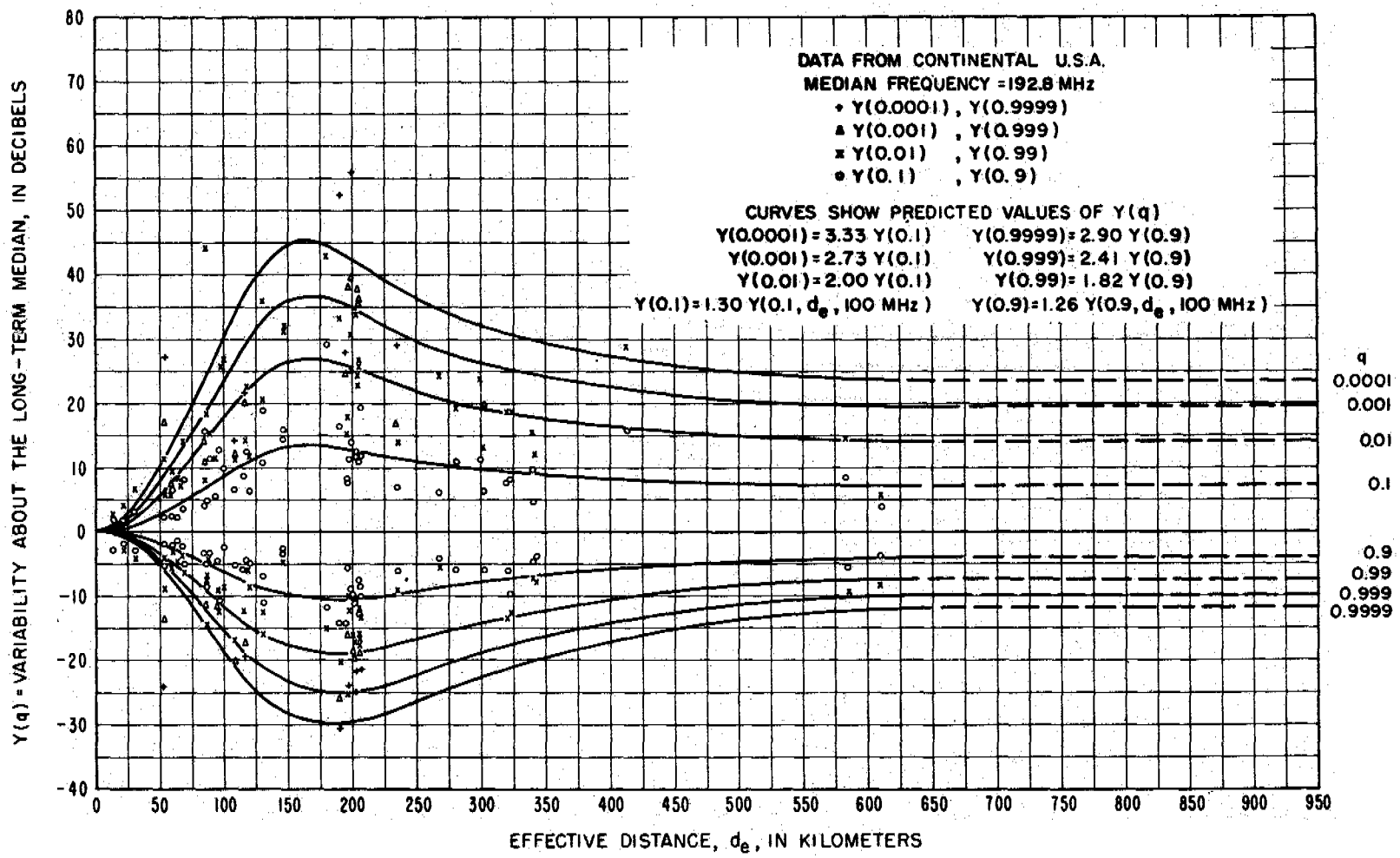

Figure 10.19

LONG-TERM POWER FADING
CONTINENTAL TEMPERATE CLIMATE, 250-450 MHz

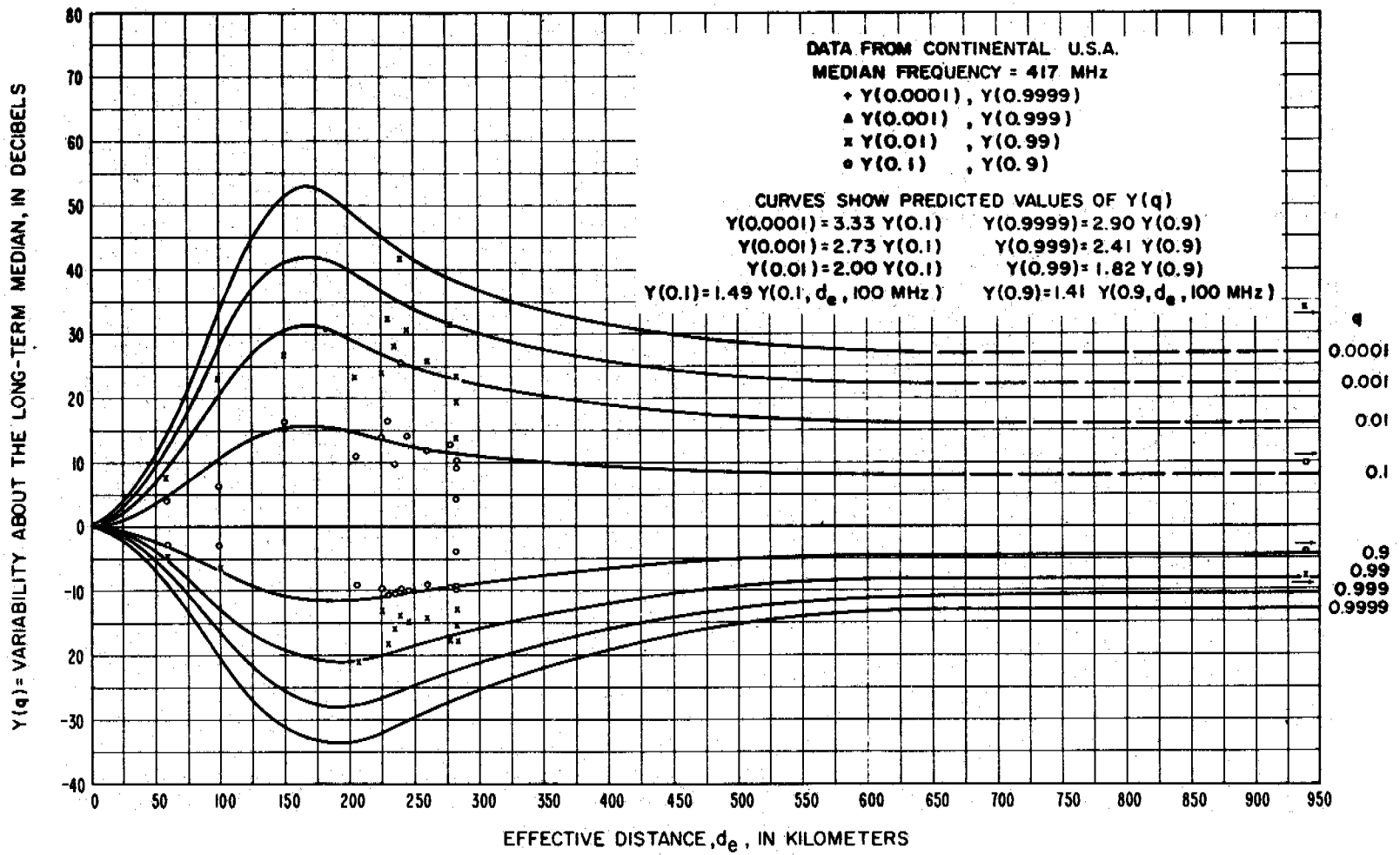

Figure 10.20

LONG-TERM POWER FADING
CONTINENTAL TEMPERATE CLIMATE, 450-1000 MHz

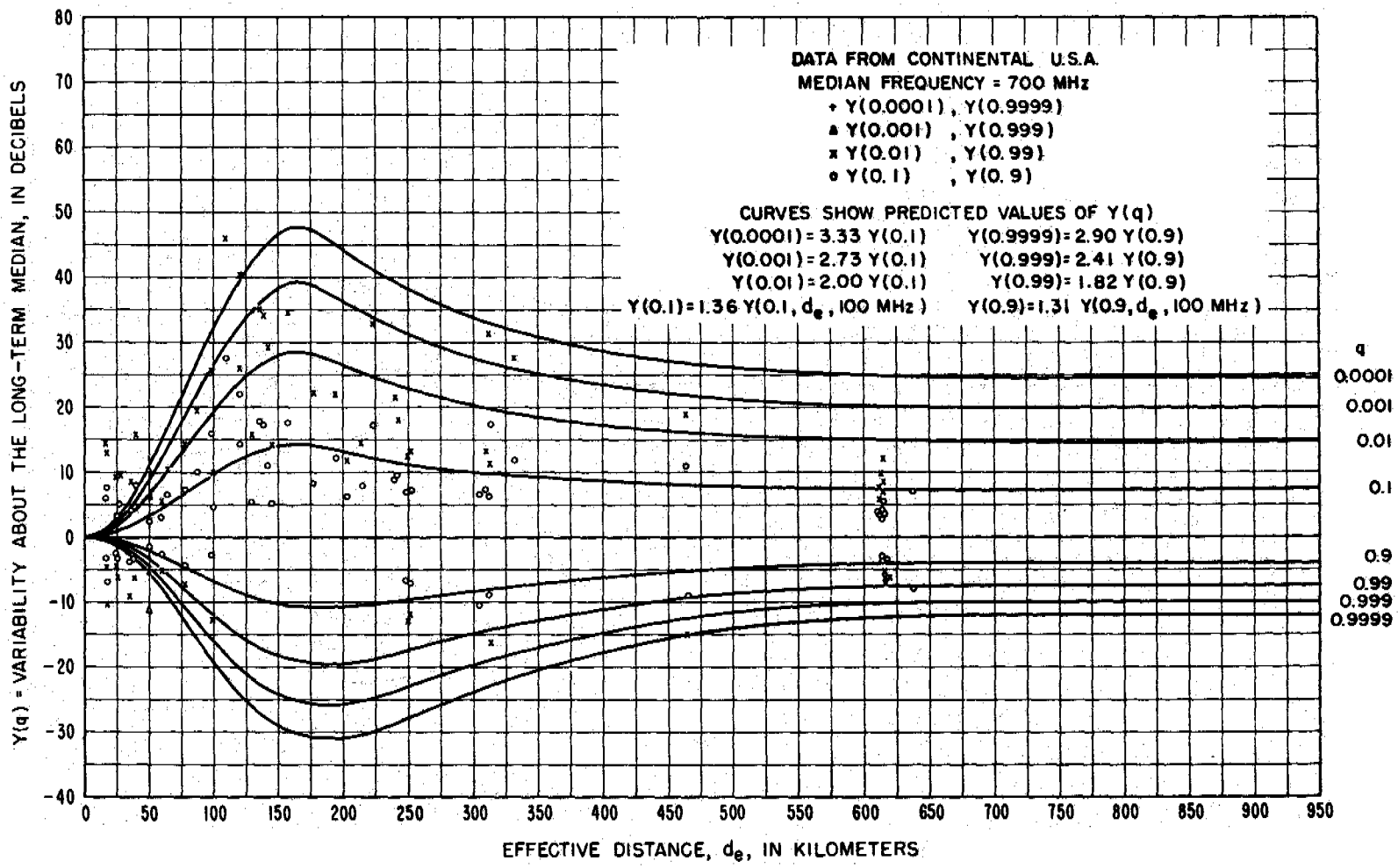

Figure 10.21

LONG-TERM POWER FADING
CONTINENTAL TEMPERATE CLIMATE, FREQ >1000 MHz

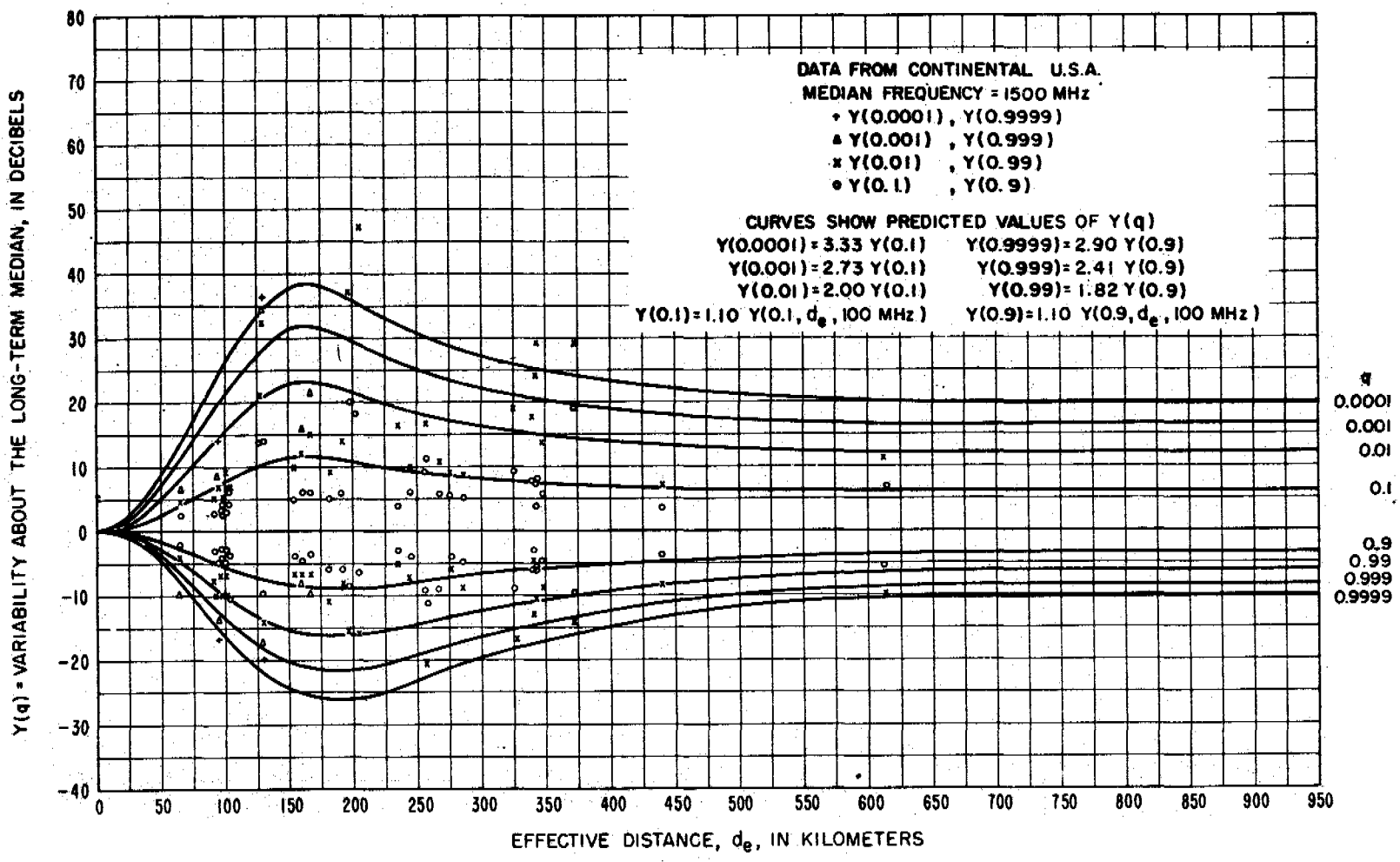

Figure 10.22

LONG-TERM POWER FADING

MARITIME TEMPERATE CLIMATE OVERLAND, BANDS I AND II (40 - 100 MHz)

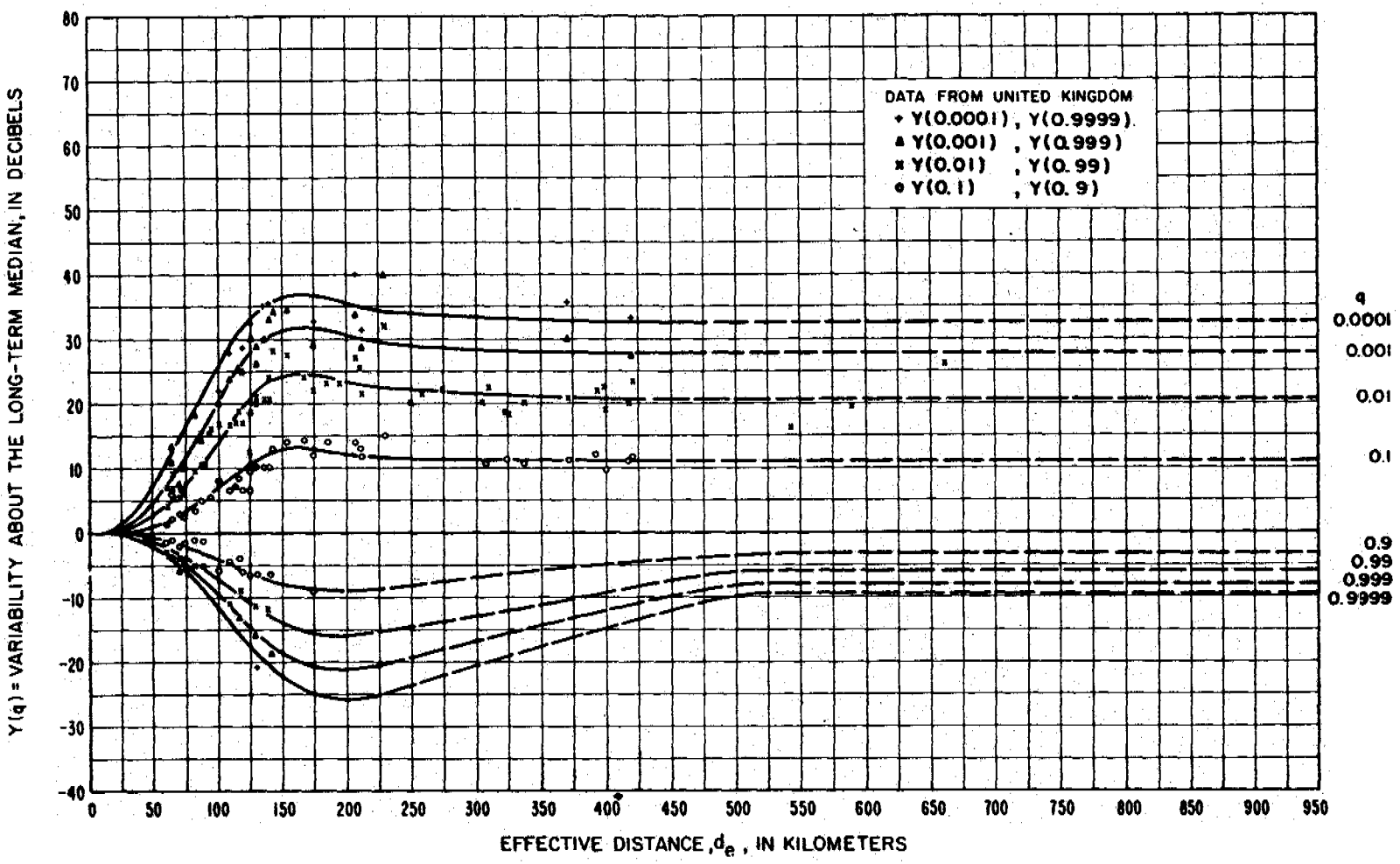

Figure 10.23

LONG-TERM POWER FADING

MARITIME TEMPERATE CLIMATE OVERSEA, BANDS I AND II (40 -100 MHz)

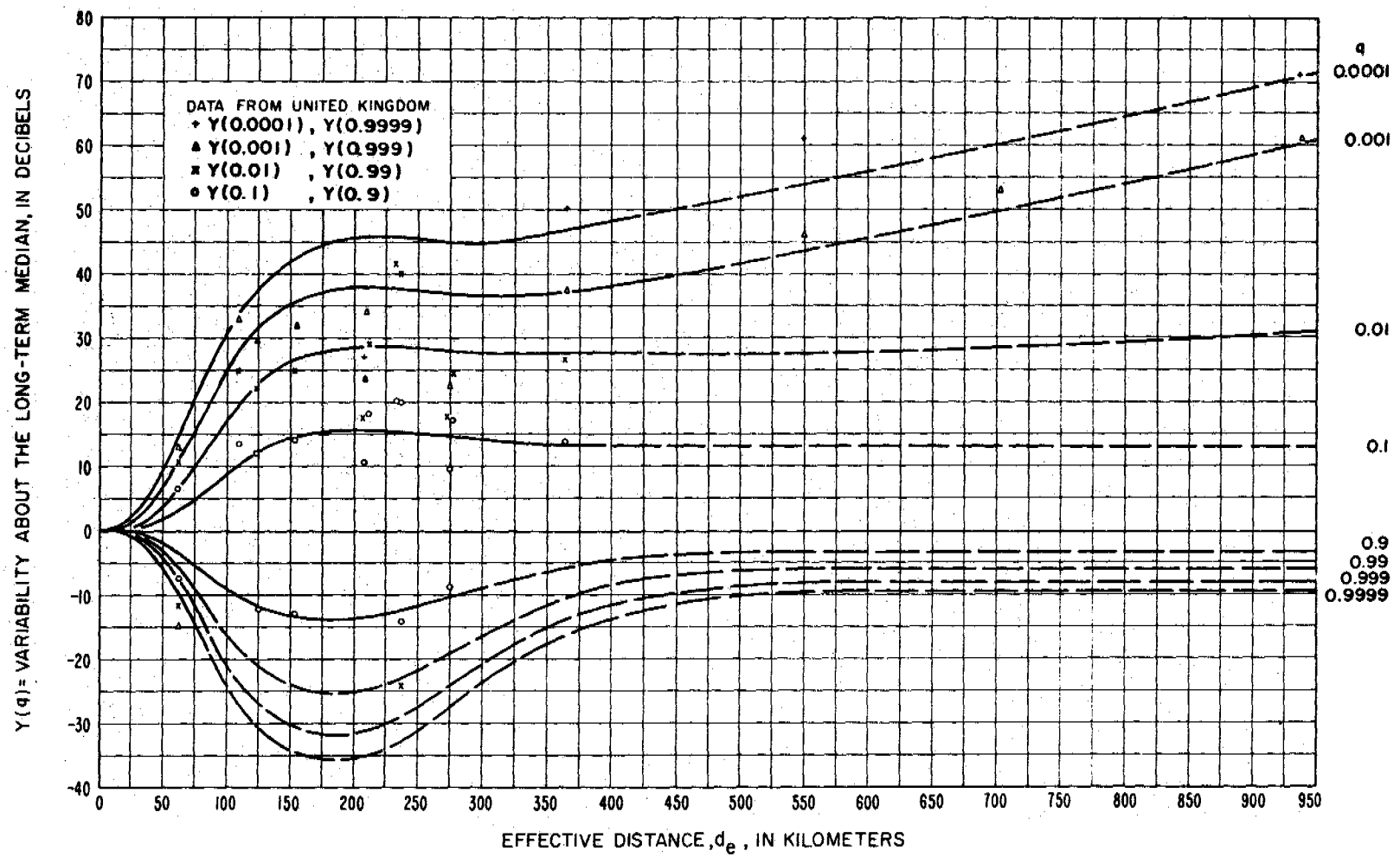

Figure 10.24

LONG-TERM POWER FADING

MARITIME TEMPERATE CLIMATE OVERLAND, BAND III (150-250 MHz)

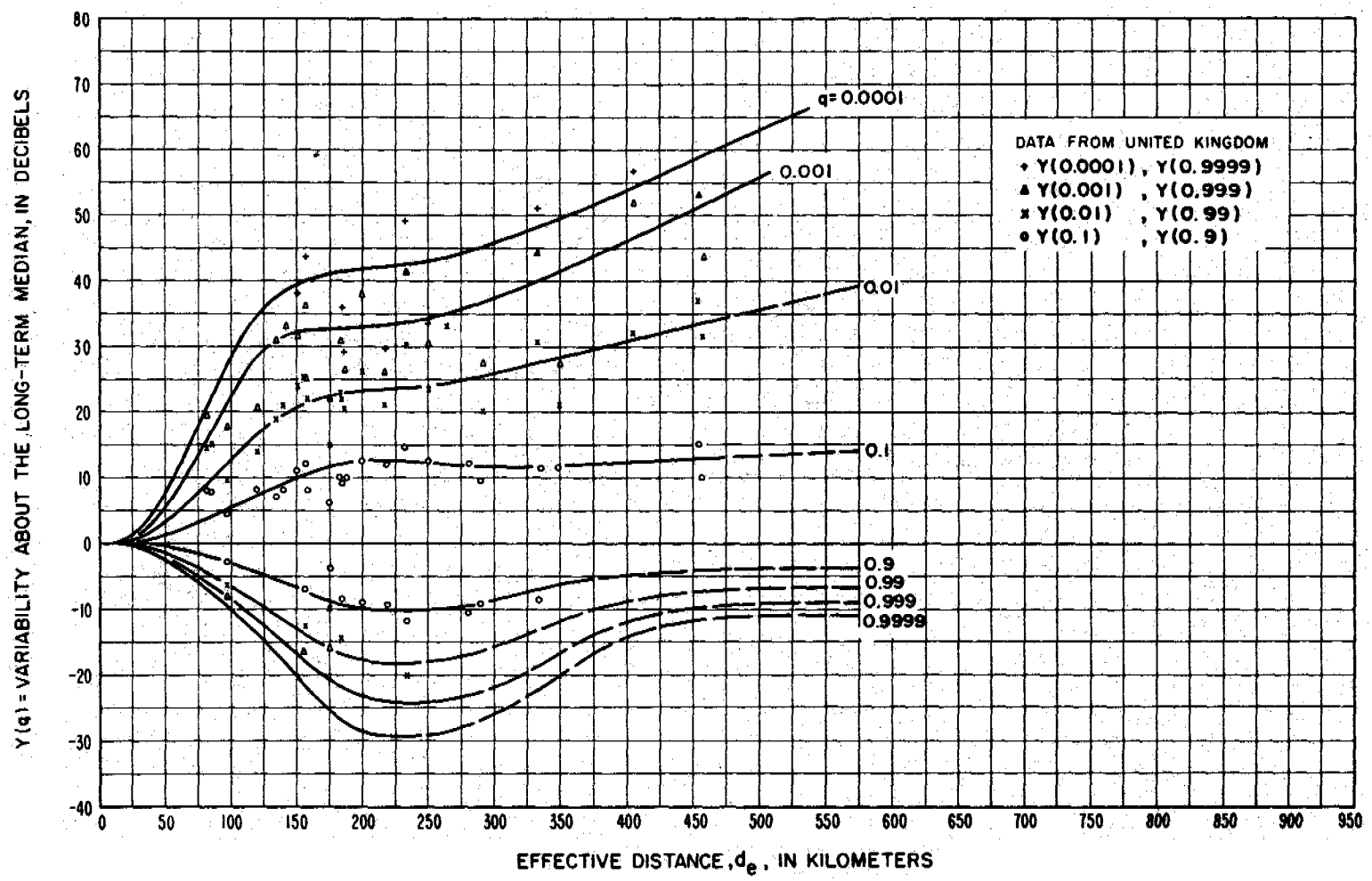

Figure 10.25

LONG-TERM POWER FADING

MARITIME TEMPERATE CLIMATE OVERSEA, BAND III (150-250 MHz)

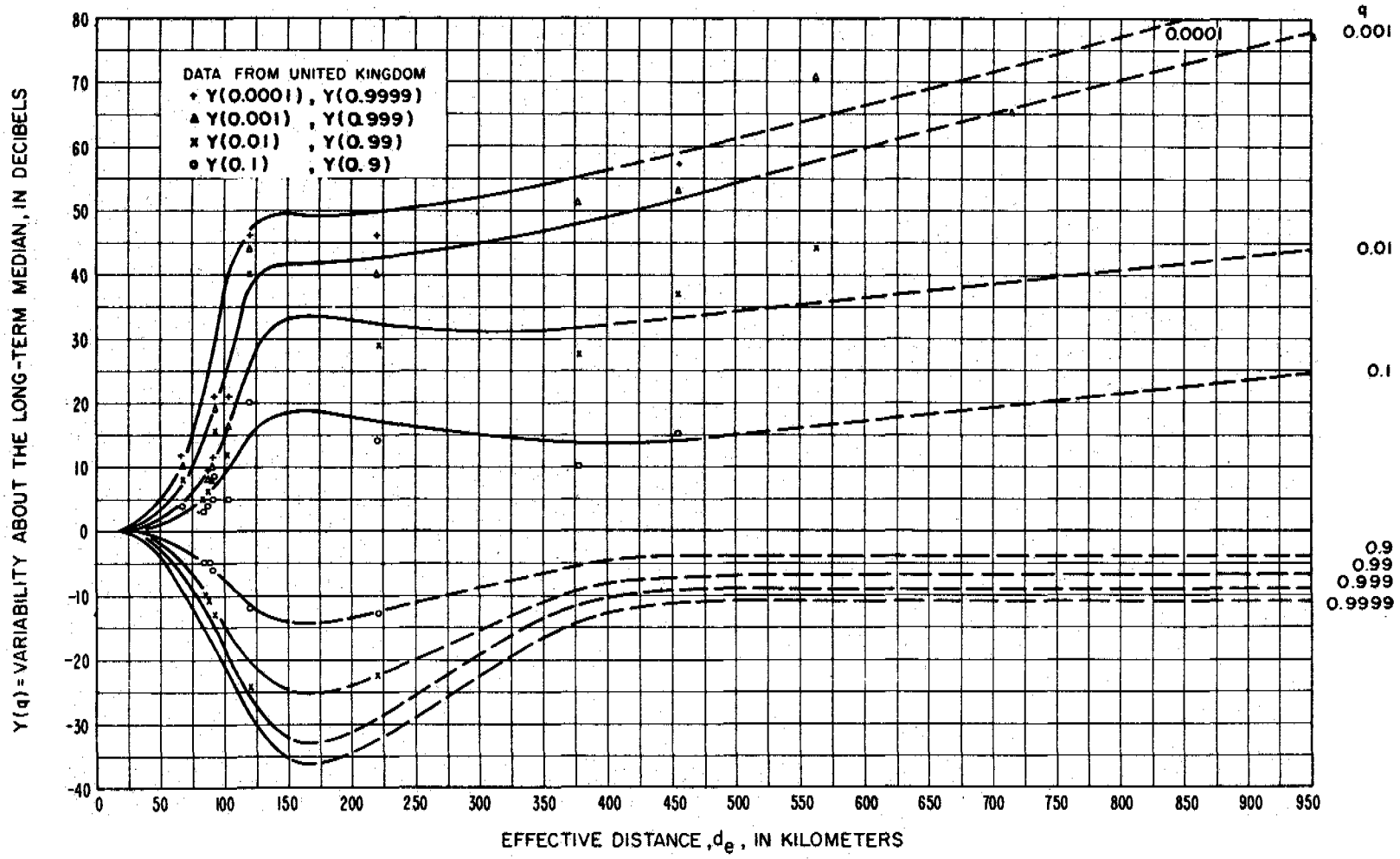

Figure 10.26

LONG-TERM POWER FADING

MARITIME TEMPERATE CLIMATE OVERLAND, BANDS IV AND V (450-1000 MHz)

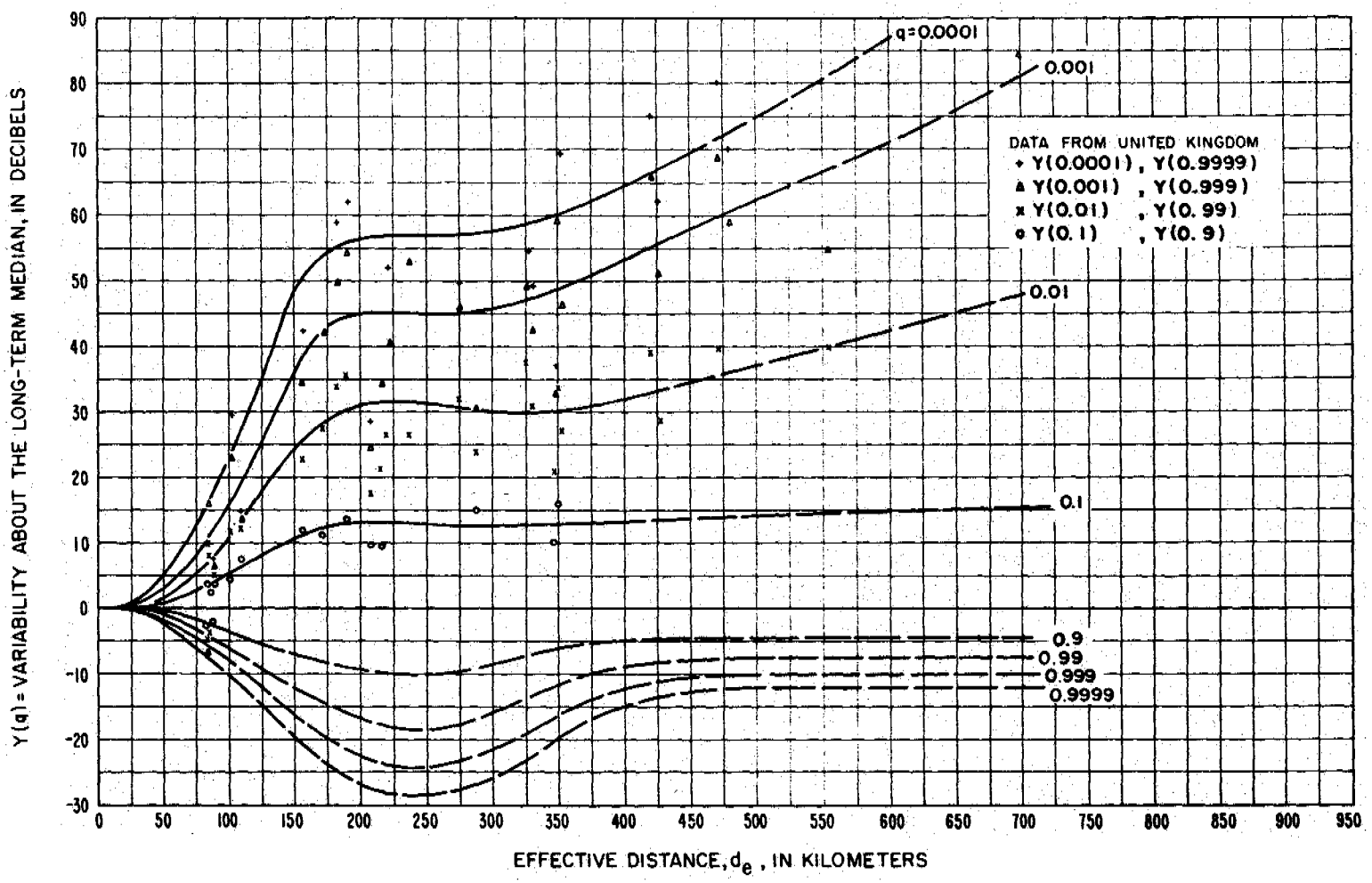

Figure 10.27

LONG-TERM POWER FADING

MARITIME TEMPERATE CLIMATE OVERSEA, BANDS IV AND V (450-1000 MHz)

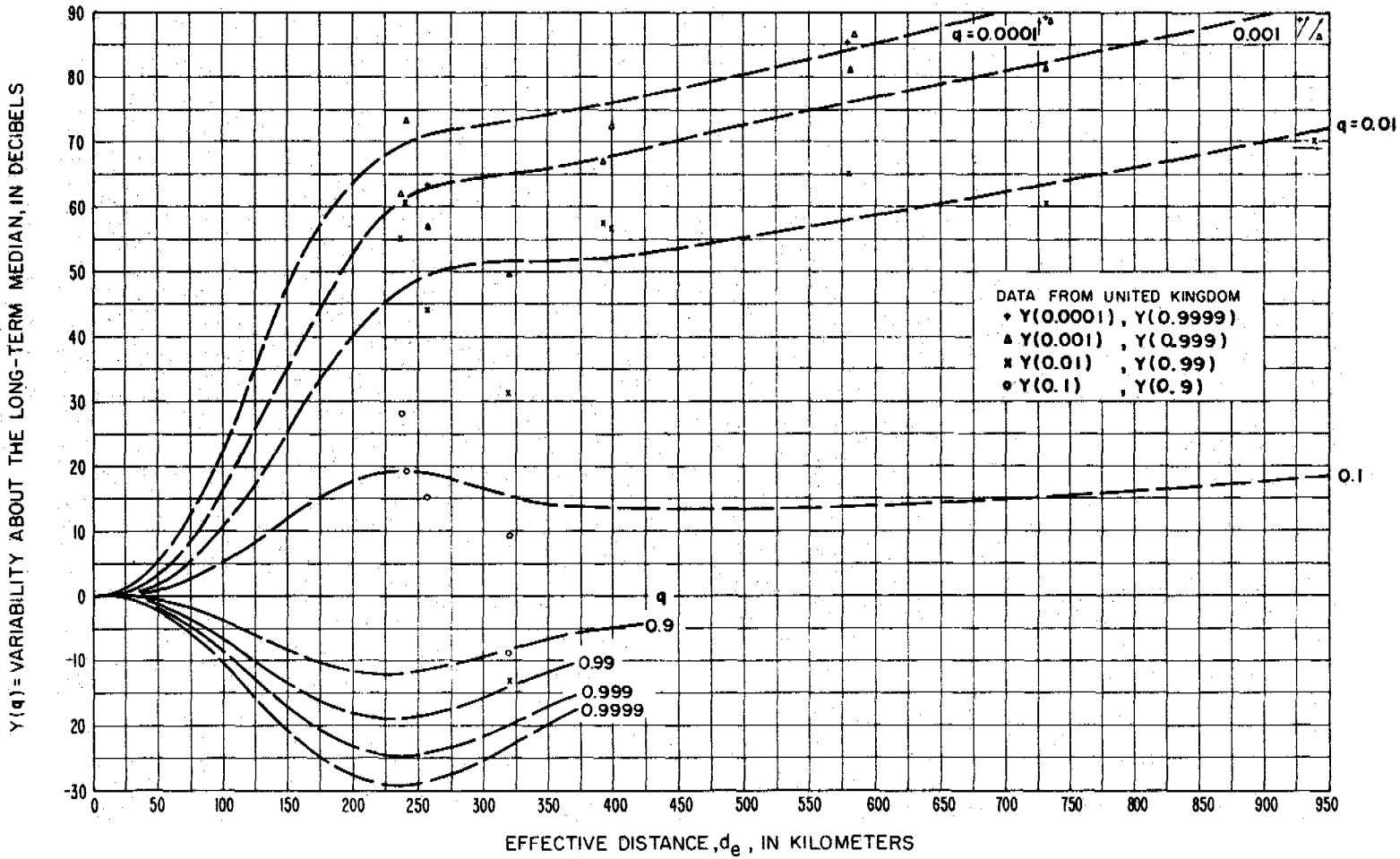

Figure 10.28